

Accurate first-principles calculations for $^{12}\text{CH}_3\text{D}$ infrared spectra from isotopic and symmetry transformations

Michaël Rey,^{1,a)} Andrei V. Nikitin,^{2,3} and Vladimir G. Tyuterev¹

¹Groupe de Spectrométrie Moléculaire et Atmosphérique, UMR CNRS 6089, BP 1039, F-51687, Reims Cedex 2, France

²Laboratory of Theoretical Spectroscopy, Institute of Atmospheric Optics, SB RAS, 634055 Tomsk, Russia

³Tomsk State University, 36 Lenin Avenue, 634050 Tomsk, Russia

(Received 14 May 2014; accepted 11 July 2014; published online 31 July 2014)

Accurate variational high-resolution spectra calculations in the range $0\text{--}8000\text{ cm}^{-1}$ are reported for the first time for the monodeuterated methane ($^{12}\text{CH}_3\text{D}$). Global calculations were performed by using recent *ab initio* surfaces for line positions and line intensities derived from the main isotopologue $^{12}\text{CH}_4$. Calculation of excited vibrational levels and high- J rovibrational states is described by using the normal mode Eckart-Watson Hamiltonian combined with irreducible tensor formalism and appropriate numerical procedures for solving the quantum nuclear motion problem. The isotopic H \rightarrow D substitution is studied in details by means of symmetry and nonlinear normal mode coordinate transformations. Theoretical spectra predictions are given up to $J = 25$ and compared with the HITRAN 2012 database representing a compilation of line lists derived from analyses of experimental spectra. The results are in very good agreement with available empirical data suggesting that a large number of yet unassigned lines in observed spectra could be identified and modeled using the present approach. © 2014 AIP Publishing LLC. [<http://dx.doi.org/10.1063/1.4890956>]

I. INTRODUCTION

Methane ($^{12}\text{CH}_4$) is a very important hydrocarbon in Earth's atmosphere and environmental sciences as it acts as a greenhouse gas.¹ It is also of major importance for the modeling of various planetary atmospheres, e.g., methane is the most abundant hydrocarbon in the atmosphere of Titan,² and for other astrophysical applications.^{3–9} Very recently theoretical hot methane line lists up to 2000 K have been constructed.¹⁰ Concerning the monodeuterated methane ($^{12}\text{CH}_3\text{D}$) though it has a quite low abundance ($\sim 6 \times 10^{-4}$), it contributes significantly to the absorption in the so-called $1.58\text{ }\mu\text{m}$ transparency windows¹¹ in planetary spectra where the opacity due to $^{12}\text{CH}_4$ is quite weak. It is also an isotopic tracer and is used to determine the H/D ratios in planetary atmospheres.^{12,13} In spite of the growing number of theoretical predictions^{14–30} for $^{12}\text{CH}_4$ from potential energy surfaces (PES) and dipole moment surfaces (DMS), there exist a relatively small number of publications devoted to the modeling of $^{12}\text{CH}_3\text{D}$ spectra using the *global* approach.^{31,32} Although one might expect that the current state of the detailed analysis for a given spectral range could reach the same precision as for $^{12}\text{CH}_4$, this is not the case. The reason is that the H \rightarrow D substitution breaks the symmetry from T_d group to C_{3v} group and consequently some degeneracies of ro-vibrational states are removed making the line-by-line analysis quite different from the major isotopologue. In addition it is the most abundant deuterio isotopologues but its spectra appear more complicated and thus more difficult to interpret and analyse than

that of CD_3H considered in Refs. 33 and 34 due to strong Fermi resonances between the stretching and bending modes. The highly excited C–H stretching vibrations of CH_3D and CD_3H were studied in the frame of the local mode theory.^{35–38} It was thus shown that in the case of CH_3D the C–H local modes strongly mix with bending normal modes.

Past and current high-resolution line-by-line analyses (in positions and intensities) for $^{12}\text{CH}_3\text{D}$ are mainly based on empirical effective polyad models using normal mode representations. These models treat all states belonging to a manifold of strongly interacting vibrational levels in a certain energy range simultaneously.^{39–45} Most of the spectroscopic data and assignments up to 5000 cm^{-1} included in the last edition of the HITRAN database^{46,47} were formed by using such polyad-by-polyad empirical models. Above 5500 cm^{-1} the new HITRAN compilation was based on spectra analyses⁴⁸ and on experimental measurements at cold and room temperature. Most of lines measured in Grenoble university with the laser cavity ring-down (CRDS) method have been compiled in the WKLMC list⁴⁹ providing also some empirical lower state energy levels. Line positions in large scale Fourier transform $^{12}\text{CH}_3\text{D}$ spectra recorded in Zurich ETH ($2900\text{--}9000\text{ cm}^{-1}$) have been partly analysed by Ulenikov *et al.*,⁵⁰ resulting in band center determination of 57 new bands and in corresponding lists of assigned transitions. However, no line intensities were reported. CRDS spectra of the C–H stretch fundamental and overtones have been recorded⁵¹ up to $16\,600\text{ cm}^{-1}$. Recently, over 1360 line intensities in the range $4000\text{--}4550\text{ cm}^{-1}$ were fitted with an effective transition moment model with a RMS of 9% that represents the best available detailed line-by-line analysis.⁴⁵ Nevertheless, numerous

^{a)}Electronic mail: michael.rey@univ-reims.fr

lines have not been reproduced at the expected accuracy whereas a large number of lines remained unassigned. Moreover, the extrapolated empirical effective models beyond fitted data fail to describe correctly spectra due to numerous interacting vibrational levels and sublevels. As discussed later, the polyad structure of CH_3D is not well-defined compared to that of methane. Consequently, some vibrational bands and resonance coupling parameters have to be added “by hand” in the model in a pragmatic way. In this context variational calculations based on PES and DMS permit accounting inherently for all possible intra-molecular interactions, including Fermi and Coriolis resonances coupling terms in a wide spectral range. A considerable progress in theoretical predictions of highly excited vibration-rotational states and transitions from *ab initio* PES and DMS as well as in improvements of computational codes for solving the Schroedinger nuclear motion equation have been recently achieved (see, for example, Refs. 26, 29, and 52–64 and references therein, the list being not exhaustive). This help resolving many issues related to the analysis of experimental spectra, particularly for methane.⁶⁵

In this work, we report global predictions of rovibrational spectra and dipole moment intensities for $^{12}\text{CH}_3\text{D}$ using our recent PES²⁶ and DMS⁶⁶ (hereafter referred to as NRT surfaces) of methane based on extended *ab initio* calculations. To explicitly account for all symmetry properties, we extend the normal-mode tensor formalism combined with variational calculations as was already used for PH_3 , $^{12}\text{CH}_4$, and $^{13}\text{CH}_4$ and permitted obtaining accurate predictions^{29,30,67} for rovibrational spectra. In order to optimize the cost of variational calculations, we have developed a truncation-reduction technique for the Hamiltonian normal mode expansion and for the basis set compression. On the other hand, we focus on the explicit derivation of formulas for the passage from T_d to C_{3v} species through symmetry considerations and nonlinear coordinate transformations in the laboratory and Eckart molecular fixed frames. Corresponding isotopic relations are thus derived.

II. COORDINATE AND SYMMETRY TRANSFORMATIONS

For this work, we start from analytical expressions for the Hamiltonian and DMS components of the main isotopologue $^{12}\text{CH}_4$ and then proceed by axes switching to derive theoretical model adapted to $^{12}\text{CH}_3\text{D}$. This is done by means of $T_d \leftrightarrow C_{3v}$ transformations. Because of mass-dependent contributions and of the symmetry breakdown, the normal-mode/Eckart frame conversion from $^{12}\text{CH}_4$ to $^{12}\text{CH}_3\text{D}$ is not direct. Computationally speaking, it turns out more convenient to first treat $^{12}\text{CH}_4$ as a particular case of C_{3v} symmetric top molecule before properly deriving theoretical expressions for $^{12}\text{CH}_3\text{D}$. Accordingly, the following transformation:

$$^{12}\text{CH}_4 (T_d) \xrightarrow{I} ^{12}\text{CH}_4 (C_{3v}) \xrightarrow{II} ^{12}\text{CH}_3\text{D} (C_{3v}) \quad (1)$$

will be explicitly considered hereafter. Useful relations corresponding to the steps *I* and *II* will be also given.

A. Laboratory and Eckart frames

1. Definitions and conventions

Let us now summarize the expressions relating the $3N$ Cartesian coordinates in the body fixed frame (BFF) to those in the laboratory fixed frame (LFF). Let \mathbf{X}_i ($i = 1, 2, \dots, N$) denote the position vector of particle i and let $(\vec{\mathcal{L}}_1, \vec{\mathcal{L}}_2, \vec{\mathcal{L}}_3)$ denote a right-handed triad of unit vectors defining a LFF. The vector components α are thus defined as $X_{i\alpha} = \vec{\mathcal{L}}_\alpha \cdot \mathbf{X}_i$, where $X_{i1} \equiv X_i$, $X_{i2} \equiv Y_i$, and $X_{i3} \equiv Z_i$. Similarly, let \mathbf{x}_i denote the vector position of the body fixed Eckart frame with unit vectors $(\vec{f}_1, \vec{f}_2, \vec{f}_3)$. The explicit construction of the Eckart frame, which coincides with principal axes frame at equilibrium, is made by means of the vectors $(\vec{F}_1, \vec{F}_2, \vec{F}_3)$ as follows:^{68–70}

$$\vec{F}_\alpha = \sum_i m_i a_{i\alpha} \mathbf{X}_i = \sum_{\alpha'} F_{\alpha'\alpha} \vec{\mathcal{L}}_{\alpha'} \quad (2)$$

where m_i is the mass of the particle i , $a_{i\alpha}$ is the reference configuration relative to the BFF and $F_{\alpha'\alpha} = \sum_i m_i a_{i\alpha} X_{i\alpha'}$. If $\mathbf{X}_{cm} = \sum_i m_i \mathbf{X}_i$ denotes the center of mass vector, then we have in frame-independent vector notation $\mathbf{X}_i = \mathbf{X}_{cm} + \mathbf{x}_i$ and we thus rewrite^{70,71} the Eckart vectors $\vec{F}_\alpha = \sum_i m_i a_{i\alpha} \mathbf{x}_i$ since $\sum_i m_i a_{i\alpha} = 0$. Following Eckart, a set of vectors fixed to the body is expressed by

$$[\vec{f}_1, \vec{f}_2, \vec{f}_3] = [\vec{F}_1, \vec{F}_2, \vec{F}_3] \mathcal{F}^{-1/2}, \quad (3)$$

where \mathcal{F} is the symmetric Gram matrix with elements $\mathcal{F}_{\alpha\beta} = \vec{F}_\alpha \cdot \vec{F}_\beta$. Here the notation of the type $[\vec{y}_1, \vec{y}_2, \vec{y}_3]$ stands for the 3×3 matrix whose columns contain the components of the three vectors \vec{y}_i . This frame is located at the center of mass \mathbf{X}_{cm} and always satisfies the relation $\sum_\alpha \vec{f}_\alpha \times \vec{F}_\alpha = \vec{0}$ which reduces to the original conditions given by Eckart⁶⁸ when substituting the \vec{F} vectors by the right-hand side of Eq. (2). Introducing the orthogonal 3×3 transformation \mathcal{S}^{-1} relating the space orientation of the LFF to the BFF, we write

$$X_{i\alpha} = X_{\alpha,cm} + \sum_\beta \mathcal{S}_{\alpha\beta}^{-1}(\theta, \phi, \chi) x_{i\beta}, \quad (4)$$

where (θ, ϕ, χ) are Eulerian angles. In the case where Eckart conditions hold, it has been shown that the matrix \mathbf{C} specifying the Eckart frame is a pure rotation matrix which is just the inverse of the familiar direction cosine matrix \mathbf{S} containing the Eulerian angles.⁷² This means that the Eckart vectors determine the orientation of the Eckart frame and that the direction cosines \mathbf{C} satisfy

$$\mathbf{C} = \mathbf{S}^{-1} = \mathbf{F}(\tilde{\mathbf{F}}\mathbf{F})^{-1/2}, \quad \mathcal{F}_{\alpha\beta} = (\tilde{\mathbf{F}}\mathbf{F})_{\alpha\beta}, \quad (5)$$

where $C_{\alpha\beta} = \vec{\mathcal{L}}_\alpha \cdot \vec{f}_\beta$ and \mathbf{F} is a matrix whose elements are the $F_{\alpha'\alpha}$ of (2); the three eigenvalues of the $\tilde{\mathbf{F}}\mathbf{F}$ matrix being chosen to be positive. Note that Eq. (5) corresponds to Eq. (3) written in matrix notation. The direction cosines could be conveniently expressed in terms of Euler angles. Now the Eckart frame has been properly defined, let us return to our initial problem. It is worth noting that the standard axis conventions between T_d and C_{3v} are not the same: the rotating frames attached to the molecule are usually defined in a different manner. As specified in the Appendix, in case of C_{3v} symmetry the quantization axis (Oz) is taken as the C_3 axis (typically

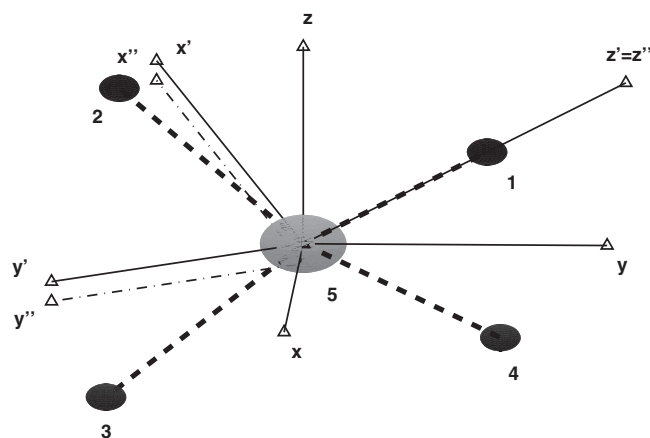


FIG. 1. Axis definition and atom numbering of a five-atomic system in its equilibrium configuration. For XY_4 molecules, the frame is (x, y, z) for T_d symmetry and (x', y', z') for C_{3v} symmetry. For XYZ molecules, the frame is (x'', y'', z'') and is deduced from (x', y', z') by an overall translation in the $-z'$ direction. For methane, $H \equiv (1, 2, 3, 4)$ and for CH_3D , $H \equiv (2, 3, 4)$ and $D \equiv (1)$.

the C-D bond for CH_3D) while for T_d symmetry, it coincides with one of the S_4 axes. The axis representation is summarized in Fig. 1 where the frames (x, y, z) and (x', y', z') are both for methane but stand for the T_d and C_{3v} , respectively. They are linked together through the rotation

$$\mathcal{R}_x = \begin{pmatrix} -\frac{1}{\sqrt{6}} & \frac{1}{\sqrt{2}} & \frac{1}{\sqrt{3}} \\ -\frac{1}{\sqrt{6}} & -\frac{1}{\sqrt{2}} & \frac{1}{\sqrt{3}} \\ \frac{2}{\sqrt{6}} & 0 & \frac{1}{\sqrt{3}} \end{pmatrix}, \quad (6)$$

and we write

$$(x', y', z')^t = \mathcal{R}_x^{-1} \cdot (x, y, z)^t. \quad (7)$$

In terms of group theory, the (x, y, z) system spans the F_2 irreducible representation (*irrep*) of T_d while (x', y') and (z') span the E and A_1 *irreps* of C_{3v} . The total angular momentum \mathbf{J} transforms as the F_1 *irrep* of T_d and spans $A_2 + E$ when subducing in C_{3v} (see Eq. (A1)). The $T_d - C_{3v}$ transformation (6) applies to the body fixed frame and does not depend of vibrational motions.

In Fig. 1, the (x'', y'', z'') frame is linked to CH_3D and is defined by a translation t over (Oz') of (x', y', z') , explicitly expressed by means of geometric considerations as

$$t = -\frac{r_e(m_D - m_H)}{\sum_i m_i} = -0.0641422, \quad (8)$$

where $r_e = 1.08601 \text{ \AA}$ is the optimized value accounting for our best *ab initio* estimations,²⁶ $m_C = 12$, $m_H = 1.00782503$, and $m_D = 2.0141017779 \text{ amu}$. The passage of Cartesian coordinates from XY_4 to XYZ systems is thus fully determined through \mathcal{R}_x . As a simple illustration, following the numbering convention of Fig. 1, the reference configuration $\mathbf{a}_i = (x_{ie}, y_{ie}, z_{ie})$ for XY_4 -type molecules in (x, y, z) transforms in $(x'', y'',$

$z'')$ for CH_3D as

$$Y(1) = (c, c, c) \quad Z(1) = (0, 0, 1.022)$$

$$Y(2) = (-c, -c, c) \quad Y(2) = (1.024, 0, -0.426)$$

$$Y(3) = (c, -c, -c) \rightarrow Y(3) = (-0.512, 0.887, -0.426)$$

$$Y(4) = (-c, c, -c) \quad Y(4) = (-0.512, -0.887, -0.426)$$

$$X(5) = (0, 0, 0) \quad X(5) = (0, 0, -0.064)$$

with $c = r_e/\sqrt{3} = 0.627$.

2. Symmetry coordinates and normal mode coordinates

In all problems of molecular physics, it is of major importance to choose an adequate set of coordinates allowing the maximum separation of the individual motions. Though the kinetic energy operator of nuclear motions takes a particularly simple form when expressed in the space-fixed Cartesian coordinates, $2T = -\hbar^2 \sum_i m_i^{-1} \partial^2 / \partial \mathbf{X}_i^2$, it is more convenient to introduce a new coordinate system which is suitable for a complete description of the individual types of motions. In the usual treatment of molecular rotations and vibrations, it is thus customary to introduce $(3N - 6)$ internal displacement coordinates \mathbf{R}_i defined as components of the vector $\mathbf{R} = (r_1, r_2, \dots; \theta_1, \theta_2, \dots)$ and the three Euler angles (θ, ϕ, χ) for the rotational coordinates (see Eq. (4)). Internal coordinates can be expressed in terms of $(3N)$ Cartesian displacements $\mathbf{d}_i = \mathbf{x}_i - \mathbf{a}_i$. Since the seminal work of Wilson,⁷³ it is common to treat semirigid nonlinear molecules having a well-defined reference structure by means of $(3N - 6)$ nonredundant, rectilinear mass-weighted normal coordinates $Q_k \in (-\infty, +\infty)$. For 5-atomic systems, they are related to \mathbf{d}_i by a linear transformation which reads^{73–76}

$$d_{i\alpha} = \sum_{k=1}^9 m_i^{-1/2} l_{i\alpha,k} Q_k \quad (i = 1 \dots 5), \quad (9)$$

where α stands for the BFF components. The orthogonality property $\sum_i \mathbf{l}_{i,k} \mathbf{l}_{i,l} = \delta_{kl}$ allows removing quadratic cross terms from the potential $V(Q)$. The \mathbf{l} transformation is obtained by diagonalizing the Hessian matrix of the potential expressed in mass-weighted Cartesian coordinates. The Eckart frame defined above presents the advantage of minimizing the vibration-rotation Coriolis coupling terms for small amplitude vibrational motions and is a quite natural choice when considering normal coordinates. The Eckart conditions are satisfied by choosing⁷⁷

$$\sum_i m_i^{1/2} \mathbf{l}_{i,k} = 0, \quad \sum_i m_i^{1/2} \mathbf{a}_i \times \mathbf{l}_{i,k} = 0. \quad (10)$$

To take full advantage of the symmetry, it is convenient to consider symmetrized normal mode $\mathbf{Q}^{(\Gamma)}$ coordinates corresponding to vibrational normal modes near the equilibrium configuration. Methane-type molecules possess nine vibrational degrees of freedom. For CH_4 spherical top, they are divided into four modes, namely, one non-degenerate mode (ν_1), one doubly degenerate mode (ν_2) and two triply

degenerate modes (ν_3, ν_4) labeled using the *irreps* Γ of T_d . For CH_3D symmetric top, they are divided into six modes, namely, three non-degenerate mode (ν_1, ν_2, ν_3) and three doubly degenerate modes (ν_4, ν_5, ν_6) labeled using the *irreps* Γ of C_{3v} . A simple way for accounting for the symmetry properties is first to construct curvilinear symmetry-adapted coordinates $S_{k\sigma}^{(\Gamma)}$ with respect to the molecular point group. They are expressed as a linear combination of the internal coordinates \mathbf{R}_i . For a given point group G , we denote by \mathbf{U} the group symmetry transformation and we thus write⁷⁵

$$\mathbf{S}_G^{(\Gamma)} = \mathbf{U}\mathbf{R}. \quad (11)$$

When making isotopic substitutions $\text{H} \rightarrow \text{D}$, the symmetry breaks down and the energy levels are classified according the *irreps* of a lower order point group G' . Using projection operators $\mathcal{P}_{R_{G'}}$, it is possible to derive the curvilinear symmetry coordinates adapted to $G \supset G'$ through a transformation \mathcal{U}_S as

$$\mathbf{S}_G^{(\Gamma)} = \mathcal{U}_S \mathbf{S}_{G'}^{(\Gamma')}. \quad (12)$$

For XY_4 ($\Gamma = A_1, E, F_2$) and XY_3Z ($\Gamma' = A_1, E$) molecules, the transformation \mathcal{U}_S is given explicitly in Eq. (A3). The normal coordinates Q also transform according to the irreps of T_d and C_{3v} and in the rectilinear approximation are related to the symmetry coordinates as

$$\left[\mathbf{S}_{T_d}^{(\Gamma)} \right]_{\text{rect}} = \mathbf{L}_{T_d} \mathbf{Q}_{T_d}^{(\Gamma)} = \mathcal{U}_S \mathbf{L}_{C_{3v}} \mathbf{Q}_{C_{3v}}^{(\Gamma')}, \quad (13)$$

where \mathbf{L} is composed of the eigenvectors of the conventional **GF** matrix of Wilson.⁷³ We can also derive the \mathbf{I}_G matrix by removing the six zero frequency normal coordinates associated with translation and rotation. The remaining $3N \times (3N - 6)$ -dimensional matrix adapted to the symmetry is expressed as

$$\mathbf{I}_G = \mathbf{M}^{-\frac{1}{2}} \tilde{\mathbf{B}} \tilde{\mathbf{L}}_G^{-1}, \quad (14)$$

where the \mathbf{B} matrix relates Cartesian and internal coordinates and \mathbf{M} is a diagonal matrix, the mass of the particles being diagonal matrix elements. In vibrational spectroscopy, it is common to define the harmonic frequencies $\omega_k = (\lambda_k^{(\Gamma)})^{1/2} / 2\pi c$, expressed in cm^{-1} , and thus to introduce dimensionless coordinates $q_{k\sigma}^{(\Gamma)} = (\lambda_k^{(\Gamma)} / \hbar^2)^{1/4} Q_{k\sigma}^{(\Gamma)}$ where $\lambda_k^{(\Gamma)}$ are the eigenvalues of the **GF** matrix associated with the k normal modes.

In the rectilinear approximation, the relation between two sets of normal coordinates is quite straightforward to establish using Eqs. (13) (or (A5)) and (A3),

$$\mathbf{q}_G^{(\Gamma)} = \mathbf{A} \mathbf{q}_{G'}^{(\Gamma')}. \quad (15)$$

From the transformation (1) we have explicitly:

- For the step *I*, that is when rotating the frame from $^{12}\text{CH}_4$ (T_d) to $^{12}\text{CH}_4$ (C_{3v}), we simply have $\mathbf{A} = \mathbf{L}_{qT_d}^{-1} \mathcal{U}_S \mathbf{L}_{qC_{3v}} \equiv \mathbf{U}_q$ where the 9×9 matrix \mathbf{U}_q is given in Eq. (A6). Here the q index in \mathbf{L} means that we work with the dimensionless coordinates.

- For the step *II*, which corresponds to the passage from $^{12}\text{CH}_4$ (C_{3v}) to $^{12}\text{CH}_3\text{D}$ (C_{3v}) we have $\mathbf{A} = \mathbf{L}_{qC_{3v}}^{-1} \mathbf{L}'_{qC_{3v}}$ where

TABLE I. Symmetry-adapted force constants $F_{ij} = \partial^2 \mathbf{V} / \partial S_{i\sigma}^{(\Gamma)} \partial S_{j\sigma}^{(\Gamma)}$ ($\text{md } \text{\AA}^{-1}$) and harmonic frequencies (cm^{-1}) for $^{12}\text{CH}_3\text{D}$ deduced from those of methane $^{12}\text{CH}_4$ using Eqs. (12), (16), (17), and (18) and $\omega_1 = 3039.56$, $\omega_2 = 1571.45$, $\omega_3 = 3162.17$, and $\omega_4 = 1344.76 \text{ cm}^{-1}$.

| | This work | | This work | Ref. 50 | Ref. 78 |
|---|-----------|------------|-----------|---------|---------|
| F_{11} | 1.513304 | ω_1 | 3075.35 | 3073.68 | 3071.40 |
| F_{12} | -0.117235 | ω_2 | 2288.54 | 2288.74 | 2285.20 |
| F_{13} | 0.011036 | ω_3 | 1339.24 | 1340.71 | 1339.80 |
| F_{22} | 0.596173 | ω_4 | 3161.89 | 3163.88 | 3156.80 |
| F_{23} | 0.101528 | ω_5 | 1508.91 | 1504.30 | 1508.10 |
| F_{33} | 1.500561 | ω_6 | 1187.76 | 1188.30 | 1188.10 |
| $F_{4\alpha 4\alpha}$ | 1.494189 | | | | |
| $F_{4\alpha 5\beta}$ | -0.117235 | | | | |
| $F_{5\alpha 5\alpha}$ | 0.596173 | | | | |
| $F_{6\alpha 6\alpha}$ | 0.648537 | | | | |
| $\alpha, \beta = a, b, \alpha \neq \beta$ | | | | | |

the primed quantities denote some isotopic species. This matrix reads for the A_1 bloc

$$\mathbf{A}(A_1) = \begin{pmatrix} -0.5619 & 0.6981 & 0.0271 \\ 0.8266 & 0.4939 & 0.0177 \\ 0.0026 & -0.0644 & 0.9967 \end{pmatrix}, \quad (16)$$

and for the (E, a) bloc

$$\mathbf{A}(E, a) = \begin{pmatrix} 0.9995 & 0.0012 & -0.0021 \\ -0.0042 & 0.9119 & -0.3180 \\ 0.0040 & 0.3875 & 0.8747 \end{pmatrix}, \quad (17)$$

the (E, b) bloc being similar. The harmonic frequencies of different isotopologues are related through \mathbf{A} as

$$I_{\omega'} = \tilde{\mathbf{A}} I_{\omega} \mathbf{A}, \quad (18)$$

where I_{ω} is a diagonal matrix which contains the ω values. The ω' values for $^{12}\text{CH}_3\text{D}$ was thus derived and are given in Table I. We clearly see from Eq. (16) that the stretching modes ν_1 and ν_2 are strongly mixed due to the heavy C-D bond. Thus the ν_2 band of $^{12}\text{CH}_3\text{D}$ could be seen as the principal counterpart of the ν_1 band of methane $^{12}\text{CH}_4$ with the frequency which goes down by 800 cm^{-1} , leading to a complex polyad structure. For practical applications, one has to consider true curvilinear coordinates which are nonlinear functions of Cartesian coordinates and consequently of normal coordinates. To this end, the definition of Eq. (13) must be extended and can be written as a power series expansion

$$\begin{aligned} S_{i\sigma}^{(\Gamma)} &= L_{q;i,j} q_{j\sigma}^{(\Gamma)} + \frac{1}{2} L_{q;i,jk} q_{j\sigma'}^{(\Gamma')} q_{k\sigma''}^{(\Gamma'')} \\ &+ \frac{1}{6} L_{q;i,jkl} q_{j\sigma'}^{(\Gamma')} q_{k\sigma''}^{(\Gamma'')} q_{l\sigma'''}^{(\Gamma''')} + \dots, \end{aligned} \quad (19)$$

with the symmetry condition $\Gamma(q_j) \times \Gamma(q_k) \times \dots \times \Gamma(q_l) \supset \Gamma$. So in the general case, the transformation of rectilinear normal coordinates between two isotopic species is written as

$$\mathbf{q}_G^{(\Gamma)} = \mathbf{A} \mathbf{q}_{G'}^{(\Gamma')} + \mathcal{G}(\mathbf{q}_{G'}^{(\Gamma')}), \quad (20)$$

where \mathcal{G} is a nonlinear function to be defined. The procedure will be explained in Sec. II B.

B. Nonlinear normal coordinate transformations

1. Analytical derivatives

Here it is supposed that we work with translationally invariant \mathbf{X}_i coordinate. The method described above allows to properly transform internal or Cartesian coordinates in normal coordinates in the frame fixed in the body. From Eqs. (4) and (9), we see that the transformation from \mathbf{X}_i to \mathbf{Q} is linear. It may also occur that the transformation from normal to Cartesian coordinates is useful. For example when only potential, dipole moment or other functions in terms of normal mode coordinates are available, a backward transformation to Cartesian coordinates is required in case of isotopic substitutions. To this end, we have to evaluate the Jacobian $\partial\mathbf{Q}/\partial\mathbf{X}_i$ with respect to space-fixed nuclear coordinates, to avoid using \mathbf{x}_i coordinates subject to six constraints. However, it is to be noted that the Jacobian matrix is not constant in that case but is a function⁷⁹ of \mathbf{Q} . As a direct consequence, such a \mathbf{Q} to \mathbf{X}_i transformation becomes nonlinear. As stated by Sutcliffe⁸⁰ “The nonlinearity is a topological consequence of any transformation that allows rotational motion to be separated.” We thus need to expand the function $\mathbf{Q}(\mathbf{X}_i)$ and evaluate the successive derivatives at the reference geometry ($Q_k = 0$). A possible way to do this is to follow Refs. 81–83, using the above considerations. From linear momenta operator transformations, Louck *et al.*⁸¹ have derived the first derivative, which will serve to compute second, third derivatives and so on. It reads

$$\frac{\partial Q_k}{\partial X_{i\alpha}} = m_i^{1/2} \vec{\mathcal{L}}_{\alpha} \cdot \mathbf{l}_{i,k} + \vec{\Omega}_{\alpha}^i \cdot \sum_r Q_r \left(\sum_j \mathbf{l}_{j,r} \times \mathbf{l}_{j,k} \right) \quad (21)$$

with the vectors

$$\begin{aligned} \mathbf{l}_{j,k} &= \sum_{\beta} l_{j\beta,k} \vec{f}_{\beta}, \\ \vec{\Omega}_{\alpha}^i &= \sum_{\gamma} \Omega_{\alpha\gamma}^i \vec{f}_{\gamma}, \end{aligned} \quad (22)$$

where

$$\Omega_{\alpha\gamma}^i = m_i (\mathbf{C} \mathbf{A}^i \mathcal{M})_{\alpha\gamma}, \quad (23)$$

with the skew-symmetric matrix⁶⁹

$$\mathbf{A}^i = \begin{pmatrix} 0 & -a_{iz} & a_{iy} \\ a_{iz} & 0 & -a_{ix} \\ -a_{iy} & a_{ix} & 0 \end{pmatrix}. \quad (24)$$

As \mathbf{A}^i is the sum of three 3×3 antisymmetric matrices, the link with the Lie algebra of SO(3) is straightforward. The symmetric matrix \mathcal{M} is defined as $[-G + \text{tr}(G)I_3]^{-1}$, with G given in Ref. 69. Noting that

$$\begin{aligned} A_{\alpha\beta}^i &= \vec{f}_{\alpha} \cdot \mathbf{a}_i \times \vec{f}_{\beta} = \sum_{\gamma} a_{i\gamma} e_{\gamma\beta\alpha}, \\ \sum_j \mathbf{l}_{j,r} \times \mathbf{l}_{j,k} &= \xi_{rk}^{\gamma} \vec{f}_{\gamma}, \end{aligned} \quad (25)$$

and that \mathcal{M} corresponds to the Wilson's $(\mathbf{I}'')^{-1}$ matrix,⁷³ the expression (21) reduces to that given in Refs. 82 and 83. Here, the ξ 's are the Coriolis coupling constants. The first derivatives can be obtained analytically and computed at the equilibrium. We thus write

$$Q_k = \sum_{i,\alpha} D_{i,\alpha}^k X_{i\alpha} + \frac{1}{2} \sum_{i',\alpha',i,\alpha} D_{i',\alpha',i,\alpha}^k X_{i'\alpha'} X_{i\alpha} + \dots, \quad (26)$$

where

$$D_{i,\alpha}^k = m_i^{1/2} l_{i\alpha,k}, \quad (27)$$

and

$$\begin{aligned} D_{i',\alpha',i,\alpha}^k &= \sum_{\beta\gamma} e_{\alpha\beta\gamma} \left[\Omega_{\alpha'\gamma}^{i'} \right]_0 D_{i,\beta}^k \\ &+ \sum_{\gamma} \left[\Omega_{\alpha\gamma}^i \right]_0 \sum_r D_{i',\alpha'}^r \xi_{rk}^{\gamma}, \end{aligned} \quad (28)$$

with

$$\left[\Omega_{\alpha\gamma}^i \right]_0 = m_i A_{\alpha\gamma}^i I_{0\gamma}^{-1} = \frac{m_i A_{\alpha\gamma}^i}{2 \sum_j (m_j a_{j\gamma}^2)}. \quad (29)$$

Expression for $[\partial^2 Q_k / \partial X_{i\alpha} \partial X_{j\beta}]$ derivatives could be also derived analytically from the following quantities taken at the reference geometry

$$\begin{aligned} \left[\frac{\partial C_{\alpha\beta}}{\partial X_{i\gamma}} \right]_0 &= \sum_{\gamma'} e_{\alpha\beta\gamma'} \left[\Omega_{\gamma\gamma'}^i \right]_0, \\ \left[\frac{\partial \Omega_{\alpha\gamma}^i}{\partial X_{i'\alpha'}} \right]_0 &= m_i \left\{ \left[\frac{\partial C_{\alpha\alpha''}}{\partial X_{i'\alpha'}} \right]_0 A_{\alpha''\gamma}^i I_{0\gamma}^{-1} + A_{\alpha\beta}^i \mathcal{M}_{\beta'\gamma'}^{i'\alpha'} \right\}, \\ \mathcal{M}_{\beta'\gamma'}^{i'\alpha'} &= I_{0\gamma'}^{-1} I_{0\beta'}^{-1} \left[\frac{\partial \mathcal{M}_{\beta'\gamma'}^{-1}}{\partial X_{i'\alpha'}} \right]_0, \end{aligned} \quad (30)$$

with, in case of spherical tops, $I_{0x} = I_{0y} = I_{0z}$. We can also note that our D 's correspond to the L 's of Ref. 82 expressed in a quite different form. Moreover, the 3×3 matrix $\Omega_{\alpha\gamma}^i$ given in Eq. (23) can be related to the matrix β of Crawford⁸⁴ used by Watson^{79,85} to derive a general molecular kinetic-energy operator as $\Omega^i = -\mathbf{C}\beta$.

Higher partial derivatives evaluated at the reference geometry are necessary but require tedious calculations and the resulting formulas could be very complicated. In Ref. 82 the analytical derivatives were tabulated up to the third order. Alternatively, we may also use Eqs. (4), (5), and (9) to express normal coordinates in terms of translationally invariant coordinates as

$$\mathbf{Q} = \tilde{\mathbf{I}} \mathbf{M}^{\frac{1}{2}} (\tilde{\mathbf{C}} \mathbf{X}_i - \mathbf{a}_i). \quad (31)$$

Using Eqs. (68) and (71) of Ref. 81 based on the fact that $\partial(\tilde{\mathbf{C}}\mathbf{C})/\partial\mathbf{X}_i = 0$, it is straightforward to show that

$$\frac{\partial C_{\alpha\beta}}{\partial X_{j\alpha'}} = \sum_{\gamma\gamma'} e_{\gamma'\beta\gamma} C_{\alpha\gamma'} \Omega_{\alpha'\gamma'}^j, \quad (32)$$

and in that case, from Eqs. (22) and (25), the first derivative of (31),

$$\frac{\partial \mathbf{Q}}{\partial \mathbf{X}_j} = \tilde{\mathbf{M}}^{\frac{1}{2}} \left(\tilde{\mathbf{C}}_{\delta_{ij}} + \frac{\partial \tilde{\mathbf{C}}}{\partial \mathbf{X}_j} \mathbf{X}_i \right), \quad (33)$$

reduces to (21). Though other derivatives could be evaluated in a recursive manner, we shall consider in the next paragraph a numerical method to compute the successive derivatives of the direction cosines. This will allow converting any normal mode operator to a Cartesian form.

2. Normal mode isotopic transformations

The nonlinear transformation described above is useful because it opens the route to the derivation of anharmonic force fields and more generally to spectroscopic constants for different isotopologues from the reference molecule.⁸⁶ In particular this allows to relate two sets of normal mode coordinates and thus to carry an operator having the Watson's form for the reference molecule to its isotopic counterpart. From Eq. (31), we write this transformation as

$$\mathbf{Q} = \tilde{\mathbf{M}}^{\frac{1}{2}} \tilde{\mathbf{C}} \mathbf{C}' (\mathbf{M}'^{-\frac{1}{2}} \mathbf{I}' \mathbf{Q}' + \mathbf{a}'_i) - \tilde{\mathbf{M}}^{\frac{1}{2}} \mathbf{a}_i, \quad (34)$$

where the primed quantities stand for some isotopic species. From the ingredients given above, the turning transformation $\tilde{\mathbf{C}} \mathbf{C}'$ now depends on \mathbf{Q}' and can be represented as a power series expansion in these coordinates. As shown in Ref. 86, the first term of Eq. (34), namely $\tilde{\mathbf{M}}^{\frac{1}{2}} ([\tilde{\mathbf{C}} \mathbf{C}']_0 \mathbf{a}'_i - \mathbf{a}_i)$, vanishes. In that case the transformation (34) can be thus rewritten in terms of dimensionless coordinates as

$$q_k = A_k^s q'_s + \mathcal{G}, \quad (35)$$

where the A_k^s coefficients are those defined in Eqs. (15)–(17) and

$$\mathcal{G} = T_k^{sp} q'_s q'_p + \dots + T_k^{sp\dots r} q'_s q'_p \dots q'_r, \quad (36)$$

is the nonlinear part of Eq. (20). The $T_k^{sp\dots r}$ coefficients are determined through the expansion of Eq. (34). To calculate the power series expansion coefficients, we need evaluating the successive derivatives of $C_{\alpha\beta}$ and $C'_{\alpha'\beta'}$ at the C_{3v} reference geometry $q'_i = 0$. Using Eq. (5), this amounts to calculate derivatives of $\mathcal{F}^{-1/2}$. Here we employ a numerical procedure to systematically account for derivatives at any orders. The direct way would consist in the computation and differentiation of the eigensolutions of \mathcal{F} which is not a trivial task. Here we propose a method for such calculations without computing any eigenvalues/eigenvectors. This procedure can be summarized as follows:

- (i) First we compute the inverse matrix $\mathcal{H} = \mathcal{F}^{-1}$ which is well-known for a 3×3 matrix.
- (ii) Then we compute the power series expansion of $\mathcal{U} = \text{COS}(\mathcal{H}^{1/2})$ which involves only integer powers of \mathcal{H} , recursively computed as $\mathcal{H}^k = \mathcal{H} \mathcal{H}^{k-1}$.
- (iii) At each step of (ii), we employ the Taylor expansion for each element of the resulting \mathcal{H}^k matrix in power series of q'_i .

- (iv) Finally, we compute the ARCCOS series of \mathcal{U} by the same procedure as in the step (iii).

This procedure is not numerically exact but allows computing derivatives of $\mathcal{F}^{-1/2}$ at a precision ε . For this work, the COS series was recursively computed up to 25th powers while the ARCCOS series was calculated up to 60th powers to reach the accuracy $\varepsilon = 10^{-10}$. By this way we are in position to convert an arbitrary normal mode T_d operator of methane to its counterpart for C_{3v} (CH_3D or CHD_3) or C_{2v} (CH_2D_2) isotopologues. Note that the procedure proposed above is not unique. For instance, to evaluate square root matrices a more rigorous linear algebra mathematical treatment could be considered from the matrix invariants and the spectral decomposition of \mathcal{F} . As a simple numerical application, we give the normal mode transformation of the first non degenerate coordinate q_1 from $^{12}\text{CH}_4$ (C_{3v}) to $^{12}\text{CH}_3\text{D}$,

$$\begin{aligned} [\text{CH}_4] &\rightarrow [\text{CH}_3\text{D}] \\ q_1^{(A_1)} &= -0.562 q_1'^{(A_1)} + 0.698 q_2'^{(A_1)} + 0.0271 q_3'^{(A_1)} \\ &\quad + 0.00074 (q_{6a}'^{(E)})^2 - 0.00061 q_{5b}'^{(E)} q_{6b}'^{(E)} \\ &\quad - 0.00059 q_{3a}'^{(E)} (q_{6a}'^{(E)})^2 - 0.000058 q_{3a}'^{(E)} (q_{4a}'^{(E)})^2 \\ &\quad + \dots \end{aligned} \quad (37)$$

Similar expressions are derived for the other coordinates. The first line of Eq. (37) is nothing but the linearized equation (15). Using Eq. (A6) we can finally build a set normal coordinates for $^{12}\text{CH}_3\text{D}$ from that of $^{12}\text{CH}_4$ (T_d). In Ref. 86, Bykov *et al.* have given the condition of existence for the $T_k^{sp\dots r}$ coefficients, that is whether $\tilde{\mathbf{C}} \mathbf{C}'$ depends on the vibrational coordinates or not. They have shown that all $T_k^{sp\dots r}$ vanish if $e_{\alpha\delta\xi} j_{\delta\xi}^\lambda = 0$ where the parameters $j_{\delta\xi}^\lambda$ are given in Eq. (49). Such a requirement occurs when isotopic substitutions do not result in the symmetry breakdown and thus no change in the center of mass of the molecular system occurs (e.g., $^{12}\text{CH}_4 \rightarrow ^{13}\text{CH}_4$ or $^{12}\text{CH}_4 \rightarrow ^{12}\text{CD}_4$). In the latter case it follows from the relations (10) that Eq. (15) holds and normal coordinates transform linearly between each isotopologue. This is illustrated, for example, by Eqs. (11) and (17) of Refs. 29 and 30.

C. Potential expansion

We use our recent NRT methane PES obtained by extensive electronic structure calculations at the CCSD(T)/pCVQZ level of the *ab initio* theory at 19 882 geometry configurations up to 20 000 cm^{-1} with subsequent corrections due to pCV5Z radial contributions and with empirical scaling of four quadratic parameters to the fundamental frequencies.²⁶ Initially, the PES has been constructed as an analytical representation adapted to the T_d point group for the main isotopologue $^{12}\text{CH}_4$. We shall convert it here to the C_{3v} representation. The NRT PES has been built as a combination of the symmetrized powers of the $\{S_{i\sigma}^{(\Gamma)}\}_{T_d}$ curvilinear coordinates. From Eq. (12), the PES is transformed and re-expressed in terms of $\{S_{i\gamma}^{(\Gamma')}\}_{C_{3v}}$, where each $S_{C_{3v}}$ is expressed as a linear combination of the

Morse-cosines-type functions in the following manner:

$$\begin{aligned}
 S_1^{(A_1)} &= (y_2 + y_3 + y_4)/\sqrt{3}, \\
 S_2^{(A_1)} &= (C_{24} + C_{23} + C_{34} - C_{12} - C_{13} - C_{14})/\sqrt{6}, \\
 S_3^{(A_1)} &= y_1, \\
 S_{4a}^{(E)} &= (y_3 + y_4 - 2y_2)/\sqrt{6}, \\
 S_{4b}^{(E)} &= (y_4 - y_3)/\sqrt{2}, \\
 S_{5a}^{(E)} &= (C_{13} + C_{14} - 2C_{12} - C_{23} - C_{24} + 2C_{34})/\sqrt{12}, \\
 S_{5b}^{(E)} &= (C_{14} - C_{13} + C_{24} - C_{23})/2, \\
 S_{6a}^{(E)} &= (-C_{13} - C_{14} + 2C_{12} - C_{23} - C_{24} + 2C_{34})/\sqrt{12}, \\
 S_{6b}^{(E)} &= (-C_{14} + C_{13} + C_{24} - C_{23})/2.
 \end{aligned} \quad (38)$$

Here $y_i = 1 - \exp[-1.9(r_i - r_e)]$ and $C_{ij} = \cos(\theta_{ij}) - \cos(\theta_e)$ where $\cos(\theta_e) = -1/3$. Finally, the potential expansion can be written as

$$V(\mathbf{R}) = \sum_{\{\mathbf{p}\}} \mathbf{F}_{\mathbf{p}} \prod_{i\sigma} \left(S_{i\sigma}^{(\Gamma_i)} \right)_{T_d}^{p_{i\sigma}} = \sum_{\{\mathbf{p}'\}} \mathbf{F}_{\mathbf{p}'} \prod_{i\gamma} \left(S_{i\gamma}^{(\Gamma'_i)} \right)_{C_{3v}}^{p'_{i\gamma}}, \quad (39)$$

where the indices σ and γ stand for components of degenerate vibrations. The component-by-component PES expansion (39) contains 1118 parameters F in the T_d representation and 2538 parameters F' if C_{3v} symmetry coordinates are used. The complete set of F' parameters is provided in the supplementary material.⁸⁷ In order to express the PES as a nonlinear function of rectilinear normal coordinates, we proceed in several steps. First, the symmetry coordinates are written in terms of Cartesian coordinates and then using Eq. (9), we obtain the final relation $V(\mathbf{R}) \rightarrow V(\text{Cart}) \rightarrow V(\mathbf{q})$. The $^{12}\text{CH}_3\text{D}$ normal mode potential is completely deduced from the main isotopologue and reads

$$V(\mathbf{q}) = \frac{1}{2} \sum_{i\sigma} \omega_i q_{i\sigma}^{2(\Gamma)} + \frac{1}{6} \sum_{i\sigma j\sigma' k\sigma''} \phi_{ijk}^{\sigma\sigma'\sigma''} q_{i\sigma}^{(\Gamma)} q_{j\sigma'}^{(\Gamma')} q_{k\sigma''}^{(\Gamma'')} + \dots \quad (40)$$

with $\mathbf{q}^{(\Gamma)} \equiv \mathbf{q}_{C_{3v}}^{(\Gamma)}$. To test the nonlinear normal to Cartesian coordinate transformation described in Sec. II B, we carried out the transformation $V(\text{Cart}) \rightarrow V(\mathbf{q})$ and then considered a backward transformation $V(\mathbf{q}) \rightarrow V(\text{Cart})$. We have thus checked that this allows obtaining the same Cartesian force constants as the initial ones.

III. ITO NORMAL MODE MODELS FOR $^{12}\text{CH}_3\text{D}$

A. Rovibrational Hamiltonian

There exist essentially two ways of deriving the normal-mode Hamiltonian for the deuterated methane. The traditional method starts from internal coordinates in the mass-independent potential representation to derive transformations using the Wilson GF procedure. The second one is probably less intuitive and direct as it is based on the transformation of the Hamiltonian of the “mother molecules” using the nonlinear relations given above. It may be also useful to make the link between components of one of the

subgroups and the irreducible tensor operator (ITO) formalism of the full T_d point group. This is helpful for a derivation of symmetry-adapted form of an effective Hamiltonian for methane polyads obtained *via* the Contact Transformation method using MOL_CT program.⁸⁸ Some examples are given in the Appendix.

1. Hamiltonian model for $^{12}\text{CH}_3\text{D}$ from internal coordinates

Here we have extended our recent work on pyramidal four-atomics⁶⁷ to five-atomic symmetric tops by using the transformations in Secs. II A 2 and II C. We will just recall briefly the methodology which has been already detailed elsewhere.^{25,67} The commonly used vibration-rotation Hamiltonian in the Eckart BFF frame for a nonlinear polyatomic molecule in normal coordinates was formulated in its most compact form by Watson.⁷⁷ It will be thus referred to as Eckart-Watson Hamiltonian (EWH) in what follows. For $^{12}\text{CH}_3\text{D}$, the EWH expressed in rectilinear dimensionless normal coordinates q reads

$$\begin{aligned}
 H(\mathbf{p}, \mathbf{q}, \mathbf{J}) &= \frac{1}{2} \sum_{k=1}^6 \sum_{\sigma} \omega_k p_{k\sigma}^{2(\Gamma)} + V(\mathbf{q}) + U_W(\mathbf{q}) \\
 &+ \frac{1}{2} \sum_{\alpha\beta} (J_{\alpha} - \pi_{\alpha}) \mu_{\alpha\beta} (J_{\beta} - \pi_{\beta}), \quad (41)
 \end{aligned}$$

where $J_{\alpha} \Leftarrow J_{\alpha}/\hbar$ and $\pi_{\alpha} \Leftarrow \pi_{\alpha}/\hbar$ are the dimensionless BFF components of the total and vibrational angular momentum, respectively. The reciprocal inertia tensor $\mu \equiv \mu(\mathbf{q})$ is a 3×3 matrix related to the $\Omega_{\alpha\beta}^i$ coefficients of Eq. (22) as

$$\mu(\mathbf{q}) = \sum_i \tilde{\Omega}^i \mathbf{m}_i^{-1} \tilde{\Omega}^i. \quad (42)$$

In Eq. (41), $V(\mathbf{q})$ is the potential function (40) and $U_W(\mathbf{q}) = -1/8 \sum_{\alpha} \mu_{\alpha\alpha}(\mathbf{q})$ is the Watson correction term⁷⁷ which has no classical analogue.

As already pointed out, for symmetric and spherical top molecules, it is highly advantageous to exploit the molecular symmetry for block-diagonalizing the Hamiltonian matrices and thus for reducing the cost of computation and memory requirements. To this end, we have introduced efficient truncation-reduction procedures for the Hamiltonian and wavefunctions to make the solutions for quantum mechanical nuclear motions tractable. For a full account of symmetry properties, the ITO formalism initially developed for spherical top effective Hamiltonians turns out to be efficient for our purpose. Computationally speaking, the tensor formalism proposed by Nikitin *et al.*⁸⁹ is very convenient for writing operators at arbitrary order. It has been recently extended to *ab initio* Hamiltonians and dipole moments normal mode expansions.⁹⁰

Here we just recall the main point of the method as the detailed construction of ITOs can be found in Ref. 89. First, we construct symmetrized powers of creation operators $\mathcal{A}^{+(l, A_1)}$ (nondegenerate modes) and $\mathcal{A}_{\sigma}^{+(lm, \Lambda)}$ (doubly degenerate modes) where (lm) specify the powers in elementary operators a^+ and a . The annihilation part is

obtained in a similar way and the creation-annihilation couplings are defined as $\mathcal{L}_i^{(A_1)} = (\mathcal{A}^{+(l'_i, A_1)} \otimes \mathcal{A}^{(l_i, A_1)})^{(A_1)}$ ($i = 1, 2, 3$) and $\mathcal{L}_j^{(\Gamma_{jv})} = (\mathcal{A}^{+(l'_j, m'_j, \Lambda'_j)} \otimes \mathcal{A}^{(l_j, m_j, \Lambda_j)})^{(\Gamma_{jv})}_{\sigma_{jv}}$ ($j = 4, 5, 6$). For the six-mode coupling scheme, the vibrational operators are then written as

$$V_{\{\mathbf{l}'\mathbf{m}'\}(\mathbf{l}\mathbf{m})\sigma_v}^{(\Lambda', \Lambda)\Gamma(\Gamma_v)} = \left(\left(\mathcal{L}_1^{(A_1)} \otimes \mathcal{L}_2^{(A_1)} \otimes \mathcal{L}_3^{(A_1)} \right)^{(A_1)} \otimes \left(\mathcal{L}_4^{(\Gamma_4)} \otimes \mathcal{L}_5^{(\Gamma_5)} \right)^{(\Gamma_{45})} \otimes \mathcal{L}_6^{(\Gamma_6)} \right)^{(\Gamma_v)}_{\sigma_v}, \quad (43)$$

where the sets $(\mathbf{l}\mathbf{m})$, Λ , and Γ stand, respectively, for $\{(l_1)(l_2)(l_3)(l_4m_4)(l_5m_5)(l_6m_6)\}$, $\{\Lambda_4\Lambda_5\Lambda_6\}$, and $\{\Gamma_4\Gamma_5\Gamma_{45}\Gamma_6\}$. In more concise notations, hermitian and anti-hermitian vibrational operators may be constructed as

$${}^\varepsilon V_{\sigma_v}^{(\Gamma_v)} = e^{i\phi} V_{\sigma_v}^{(\Gamma_v)}, \quad (44)$$

for diagonal operators with $(\mathbf{l}'\mathbf{m}') = (\mathbf{l}\mathbf{m})$ and $\Lambda' = \Lambda$ and as

$${}^\varepsilon V_{\sigma_v}^{(\Gamma_v)} = e^{i\phi} \left(V_{\sigma_v}^{(\Gamma_v)} + \varepsilon \left(V_{\sigma_v}^{(\Gamma_v)} \right)^+ \right), \quad (45)$$

otherwise. Here ε denotes the parity of the operator. The phase factor $e^{i\phi}$ depends on the parity and is set to $e^{i\phi} = i$ for odd operators ($\varepsilon = -$) and to 1 otherwise ($\varepsilon = +$). Following the coupling scheme introduced by Moret-Bailly⁹¹ and Zhilinskii,⁹² the symmetry-adapted rotational operators read

$$R_{\sigma_r}^{\Omega(K, |k|, \Gamma_r)} = {}^{(K)}G_{\Gamma_r \sigma_r}^k R_k^{\Omega(K)} + {}^{(K)}G_{\Gamma_r \sigma_r}^{-k} R_{-k}^{\Omega(K)}, \quad (46)$$

where $R_k^{\Omega(K)}$ designate rotational spherical tensor operators of degree Ω in J_α and of rank K in $O(3)$. \mathbf{G} refers to the orientation matrix. Since the Hamiltonian must be hermitian and invariant under time-reversal, the operators V and R have necessarily the same parity in elementary momentum operators resulting to $\varepsilon = (-1)^\Omega$.

All the theoretical ingredients for transforming the EWH (41) to its tensorial counterpart in a systematic way have been implemented in our computer code TENSOR. We write this transformation for C_{3v} molecules as

$$\text{EWH} \rightarrow H(\mathbf{a}^+, \mathbf{a}, \mathbf{J}) = \sum_{\{i\}} t_{\{i\}} \left({}^\varepsilon V^{(\Gamma)} \otimes R^{\Omega(K, |k|, \Gamma)} \right)^{(A_1)}, \quad (47)$$

where the parameters t are determined algebraically from the PES and kinetic energy operator normal mode expansions. The formulation (47) is particularly useful for non-Abelian point groups because the components on degenerate *irreps* are rearranged into a more compact form. Moreover, all vibration-rotation resonance terms allowed by symmetry selection rules are systematically taken into account for a given order. The key feature of this procedure is that all degeneracies are strictly treated. Due to the symmetry breaking a part of degeneracies is removed, the number of symmetry allowed terms in (47) at a given order being larger than in the methane T_d case. For example, at order 6, the number of terms is approximately four times bigger for $^{12}\text{CH}_3\text{D}$ compared to methane $^{12}\text{CH}_4$.

2. Hamiltonian model for $^{12}\text{CH}_3\text{D}$ deduced from T_d normal coordinates of the “mother” isotopologue $^{12}\text{CH}_4$

Both mass-dependent normal coordinates and the choice of axes are different for the two isotopologues. For this reason, the relation between the corresponding EWH expansions is not trivial, particularly in the case of symmetry breaking isotopic substitutions. In order to establish these links for an arbitrary order, we start directly from the tensor model derived for $^{12}\text{CH}_4$ in Refs. 25, 29, and 30 where a form similar to (47) was derived and apply the transformation scheme (1). We skip here technical details since for this work we have built our Hamiltonian model following Sec. III A 1.

The T_d rotational operators R_{T_d} (26) of Ref. 25 can be conveniently transformed in the C_{3v} frame from the transformation properties of the total angular momentum. By this way each R_{T_d} can be related to the rotational operators (46) in the following manner:

$$\begin{aligned} [T_d] &\rightarrow [C_{3v}] \\ R_{x/y}^{1(1, F_1)} &\rightarrow \frac{1}{\sqrt{3}} R^{1(1, 0A_2)} + / - \frac{1}{\sqrt{2}} R_a^{1(1, 1E)} + \frac{1}{\sqrt{6}} R_b^{1(1, 1E)} \\ R_z^{1(1, F_1)} &\rightarrow \frac{1}{\sqrt{3}} R^{1(1, 0A_2)} - \sqrt{\frac{2}{3}} R_b^{1(1, 1E)} \\ R_\alpha^{2(2, E)} &\rightarrow -\sqrt{\frac{2}{3}} R_\alpha^{2(2, 1E)} - \frac{1}{\sqrt{3}} R_\alpha^{2(2, 2E)} \\ R_{x/y}^{2(2, F_2)} &\rightarrow \frac{1}{\sqrt{3}} R_\alpha^{2(2, 0A_1)} - \frac{1}{3\sqrt{2}} R_a^{2(2, 1E)} + / - \frac{1}{\sqrt{6}} R_b^{2(2, 1E)} \\ &\quad + \frac{1}{3} R_a^{2(2, 2E)} - / + \frac{1}{\sqrt{3}} R_b^{2(2, 2E)} \\ R_z^{2(2, F_2)} &\rightarrow \frac{1}{\sqrt{3}} R_\alpha^{2(2, 0A_1)} + \frac{\sqrt{2}}{3} R_a^{2(2, 1E)} - \frac{2}{3} R_a^{2(2, 2E)}. \end{aligned} \quad (48)$$

From the nonlinear relation (35), we could also show that each T_d vibrational operator V_{T_d} (23) of Ref. 25 is expressed as a sum of operators V (43), where for a given order the sum will run over all $(\mathbf{l}\mathbf{m})$ and $(\mathbf{l}'\mathbf{m}')$. Accordingly the normal mode tensor formulation could be directly transposed from methane (T_d) to $^{12}\text{CH}_3\text{D}$,

$$\left({}^\varepsilon V_{T_d}^{(\Gamma)} \otimes R_{T_d}^{(\Gamma)} \right)^{(A_1)} = \sum_{\{i\}} \mathcal{C}_{\{i\}} \left({}^\varepsilon V_{C_{3v}}^{(\Gamma)} \otimes R_{C_{3v}}^{\Omega(K, |k|, \Gamma)} \right)^{(A_1)}, \quad (49)$$

where the coefficients \mathcal{C} are evaluated numerically from all previous transformations.

B. Transformation of the dipole moment components

The calculation of accurate dipole moment transitions requires the use of an analytical DMS representation. For this work, we have considered the *ab initio* NRT DMS⁶⁶ whose analytical form has been initially constructed for the main isotopologue $^{12}\text{CH}_4$. The dipole moment is a polar vector and transforms according to the *irrep* $D^{(1_u)}$ of the full rotation group $O(3)$ and for tetrahedral molecules the μ_θ^m ($\theta = x, y, z$) molecule-fixed Eckart components transform according to the F_2 symmetry. Originally, for the calculation of CH_4 spectra,^{30,66} the MFF dipole moment μ_z^m component has been fitted to *ab initio* points using the sixth order

polynomial expansion in symmetry-adapted (T_d) normal mode coordinates

$$\mu_z^m[T_d] = \sum_i d_i q_{iz}^{(F_2)} + \sum_{i\sigma, j\sigma'} d_{i\sigma, j\sigma'} q_{i\sigma}^{(\Gamma)} q_{j\sigma'}^{(\Gamma')} + \dots \quad (50)$$

with $\Gamma \times \Gamma' \times \dots \supset F_2$ and contains 1053 parameters. The x and y components were deduced from Eq. (50) by symmetry considerations and contain 1176 parameters. In order to compute intensities, the DMS components were converted to ITOs adapted to T_d . For the main $^{12}\text{CH}_4$ isotopologue, our potential energy and dipole moment surfaces have been validated²⁹ via comparison on extensive rovibrational spectra calculations with experimental data for various temperatures in the range 0–9300 cm^{-1} . Also a $^{12}\text{CH}_4$ line list has been generated¹⁰ up to 2000 K in the infrared range [0–5000] cm^{-1} for astrophysical applications. The intensity errors have been estimated to be of the order of $\sim 5\%$ at least for strong and medium lines. The T_d isotopic species $^{13}\text{CH}_4$ and $^{12}\text{CD}_4$ were also considered^{29,30} by transforming the (x, y, z) normal mode components using Eq. (15). The agreement between observed and *ab initio* lines was of the same quality as for the major isotopologue $^{12}\text{CH}_4$.

To derive the dipole moment components for $^{12}\text{CH}_3\text{D}$ in normal coordinates and in appropriate axes without fitting any parameters, the procedure is less trivial than in the case of symmetry conserving substitutions and could be also summarized by the scheme of Eq. (1).

- The step *I* consists in converting in C_{3v} axes the μ_θ^m components which were initially adapted to T_d axes. According to Eq. (6), the C_{3v} components transform linearly from the T_d ones as

$$(\mu_a^{(E)}, \mu_b^{(E)}, \mu^{(A_1)})^t = \mathcal{R}_x^{-1} \cdot (\mu_x^{(F_2)}, \mu_y^{(F_2)}, \mu_z^{(F_2)})^t, \quad (51)$$

and the C_{3v} normal coordinates for methane are derived from Eq. (A5). We obtain 2365 and 2428 operators for A_1 and $(E, 1)$ components, respectively, by this purely algebraic transformation without any fit of parameters.

- In the step *II*, we substitute the nonlinear normal mode coordinate transformation (35) into Eq. (50) to obtain

$$\mu_z^m(\mathbf{q})[\text{CH}_4, T_d] \rightarrow \mu_z^m(\mathbf{q}')[\text{CH}_3\text{D}, C_{3v}]. \quad (52)$$

A form similar to Eq. (50) is thus derived for $^{12}\text{CH}_3\text{D}$ by symmetry and coordinates transformations only.

To be consistent with our Hamiltonian formulation, we also exploit the C_{3v} symmetry for the dipole moment operators by means of ITOs. As for Eq. (47), the TENSOR code was used to convert the μ_θ^m components to the symmetry-adapted ITO form

$$\mu_\theta^m(\mathbf{q}')[C_{3v}] \rightarrow \mu_\theta^m(\mathbf{a}^+, \mathbf{a}) \equiv \mu_\theta^{(\Gamma)} = \sum_{\{i\}} \mu_{\{i\}}^{(+)} V_\theta^{(\Gamma)}, \quad (53)$$

with $\Gamma = A_1, E$. Our method allows building systematically normal mode ITO models up to a given order, e.g., the sixth order $A_1 + E$ model both in (p, q) and (a^+, a) representations. These algebraic transformations are quite involved but straightforward leading finally to 34 466 symmetry allowed terms in (a^+, a) representation (53). We were able relating the DMS d parameters as those given in the expansion (50) to the

$\mu_{\{i\}}$'s in Eq. (53) in an exact way, i.e., without any fitting procedure. As an illustration we give the exact expression of some tensor operators as a function of the initial parameters. The μ_x^m and μ_z^m components can be cast into the form

$$\begin{aligned} \mu_x^m &= \mu_1^x (+) V_{\{(10)_6\}\{0\}}^{(E, A_1)_6 A_1 A_1 E(E)} \\ &+ \mu_2^x (+) V_{\{(1)_1\}\{(10)_6\}}^{(A_1, A_1)_1 (A_1, E)_6 A_1 A_1 E(E)} \\ &+ \mu_2^x (+) V_{\{(10)_4\}\{(10)_5(10)_6\}}^{(E, A_1)_4 (A_1, E)_5 (A_1, E)_6 E E A_2 E(E)} \\ &+ \dots \end{aligned} \quad (54)$$

and

$$\begin{aligned} \mu_z^m &= \mu_1^z (+) V_{\{(1)_1\}\{0\}}^{(A_1, A_1)_1 A_1 A_1 A_1 (A_1)} \\ &+ \mu_2^z (+) V_{\{(10)_6\}\{(10)_6\}}^{(E, E)_6 (A_1 A_1 A_1 A_1 A_1)} \\ &+ \mu_2^z (+) V_{\{(30)_6\}\{0\}}^{(A_1, A_1)_3 A_1 A_1 A_1 A_1 (A_1)} \\ &+ \dots \end{aligned} \quad (55)$$

with

$$\begin{aligned} \mu_1^x &= \frac{1}{\sqrt{2}} d_{6a} + \frac{1}{2\sqrt{2}} d_{6a, 6b, 6b} + \frac{3}{2\sqrt{2}} d_{6a, 6a, 6a} + \dots \\ \mu_2^x &= \frac{1}{2} d_{1, 6a} + \dots \\ \mu_3^x &= \frac{1}{4} d_{4b, 5a, 6b} - \frac{1}{4} d_{4a, 5b, 6b} + \dots \\ \mu_1^z &= \frac{1}{\sqrt{2}} d_1 + \frac{1}{2\sqrt{2}} d_{1, 6a, 6a} + \frac{3}{2\sqrt{2}} d_{1, 1, 1} + \dots \\ \mu_2^z &= \frac{1}{\sqrt{2}} d_{6a, 6a} + \frac{1}{\sqrt{2}} d_{6b, 6b} + \dots \\ \mu_3^z &= \frac{\sqrt{3}}{4} d_{6a, 6b, 6b} - \frac{\sqrt{3}}{4} d_{6a, 6a, 6a} + \dots \end{aligned}$$

For the sake of simplicity, we have followed notations of Ref. 25 by setting $(l_i m_i) = (lm)_i$ if $l_i + m_i > 0$ and 0 otherwise. Similarly, (Λ'_i, Λ_i) was denoted by $(\Lambda', \Lambda)_i$ and omitted if $l_i + m_i + l'_i + m'_i = 0$.

IV. AB INITIO ROVIBRATIONAL SPECTRA

A. Energy level calculations

In order to compute vibration-rotation energy levels, we need first to build a basis set by employing the same inner coupling scheme than that of the Hamiltonian (47). The simplest way consists in using direct product of 1D primitive harmonic oscillator functions. The 9D vibrational primitive functions $\Phi_{v\sigma_v}^{(C_v)}$ are thus built as a tensor product of three one-dimensional harmonic oscillator functions $\Phi_{v_i}^{(A_1)}$ ($v_i = 1, 2, 3$) with three two-dimensional ones $\Phi_{v_i}^{(E)}$ ($v_i = 4, 5, 6$). For $J > 0$, a set of rovibrational basis functions is obtained by the coupling between vibrational and rotational functions

$$\Phi_{v, M, \sigma}^{(J, C)} = \left(\Phi_v^{(C_v)} \otimes \Phi_M^{(J, K, C_r)} \right)_\sigma^{(C)}, \quad (56)$$

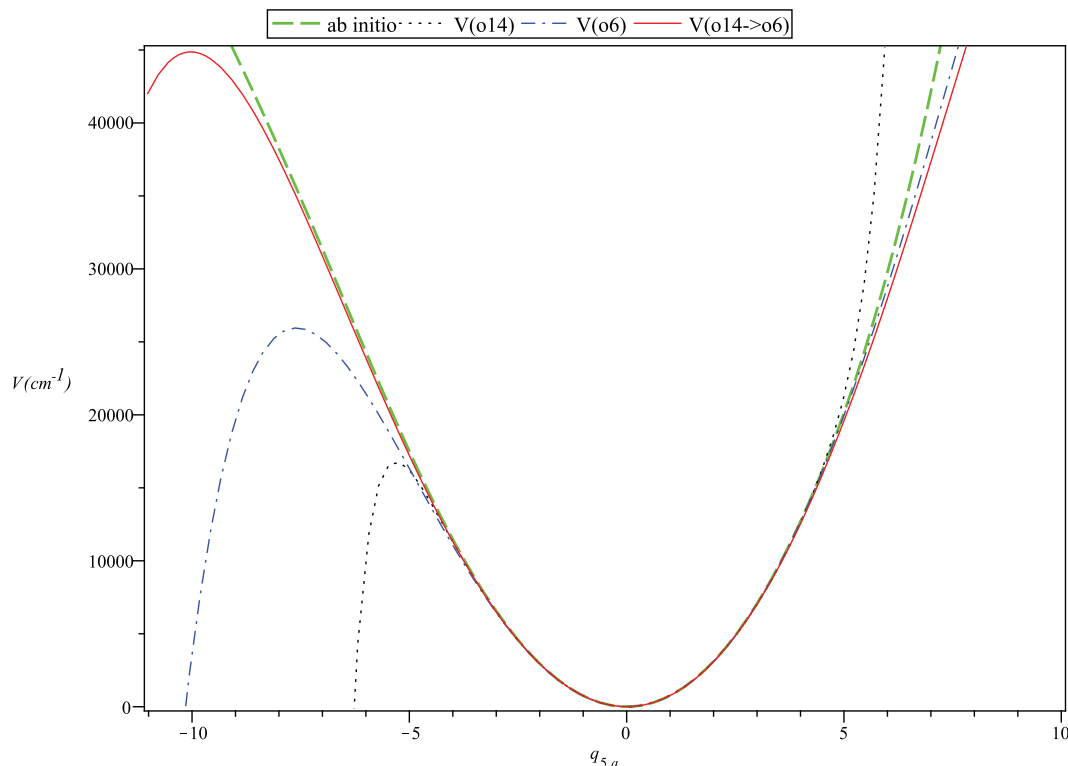


FIG. 2. One-dimensional PES cut along the bending coordinate component q_{5a} for the Taylor expansions $V(o6)$ (dotted curve), $V(o14)$ (dashed-dotted curve) and for the reduced $14 \rightarrow 6$ (solid curve) potential. The original “*ab initio*” NRT potential (39) is given in dashed curve. It is seen that the reduction procedure improves upon Taylor expansion pushing non-physical features beyond the dissociation threshold (see text).

where according to Eq. (46), the symmetry-adapted rotational functions are constructed with the G coefficients. As already suggested in previous works, only a limited set of primitive functions is chosen through the cutoff criterium

$$F_{\kappa}(v_{\max}) \Leftrightarrow \sum \kappa_i v_i \leq v_{\max}, \quad (57)$$

with $v_i = 0, \dots, v_{\max}$ and where κ_i are some weight coefficients. The latter ones are defined in a way to optimize the number of stretching and bending basis functions. If all κ_i equal to 1, the basis will be simply denoted as $F(v_{\max})$. Alternative “pruning schemes” for defining basis-sets have been employed for example in Refs. 93–95.

An accurate global calculation of methane-type spectra remains a challenge, both in terms of CPU time and computational memory but also for converging high- J rovibrational states on a wide spectral range. In particular, the knowledge and the determination of accurate eigensolutions is of prior importance for predicting reliable line strengths. The main limitations of the normal mode approach are mainly due to (i) the drawbacks of the Taylor expansions for many degrees of freedom with an exponentially growing number of terms and (ii) the high dimensionality of the rovibrational matrices as J increases, even if the molecular symmetry is fully accounted for. In Refs. 25 and 29 we have proposed two ways for minimizing the impacts of (i) and (ii) issues by means of an efficient truncation-compression procedure which aims at optimizing the cost of the computations. This can be summarized as follows:

- *Reduction-truncation of the Hamiltonian expansion.*

For the consistency with previous calculations on methane,

the potential part as well the Watson term were first developed up to the order 14 in \mathbf{q} while the reciprocal μ tensor was developed up to the order 8. The 8th order expansion of μ proved to be sufficient leading in fact to the maximum 12th power of elementary vibrational operators in the vibrational kinetic energy part $\pi \mu \pi$. The effect of the truncation of the μ -expansion on the vibrational energy levels was studied in details for $^{12}\text{CH}_4$ in Ref. 25. The same study was done for $^{12}\text{CH}_3\text{D}$ with the rms deviation between the contributions of 6th and 8th orders up to 5000 cm^{-1} less than 10^{-3} cm^{-1} . This is clearly below the accuracy of the PES. At this stage the full EWH $H^{(14)}(\mathbf{p}, \mathbf{q}, \mathbf{J})$ contains more than 3 400 000 elementary operators requiring a large amount CPU time for the computation of matrix elements. This makes the problem intractable for large basis sets. To get around such difficulties, we have applied the reduction technique described in Ref. 29 in order to transform the initial 14th order EWH to a 6th order reduced Hamiltonian almost without degrading the accuracy. A technically efficient way to implement this reduction is using the (a^+, a) representation. The resulting Hamiltonian $H_{\text{red}}^{(14 \rightarrow 6)}(\mathbf{p}, \mathbf{q}, \mathbf{J})$ contains 32 461 elementary operators only. The computational demand is thus scaled by 1:100 at this stage. In order to build the reduced ITO form (47), only the 6th order terms were selected using the second-quantization procedure. The resulting Hamiltonian finally contains 24 048 contributions in the tensor form, scaling down the number of terms in the initial 14th order expansion by a factor 1:140. In addition, this reduction technique based on the construction of creation/annihilation operators helps also avoiding certain problems of unstable behaviors inherent to high order polynomials. This is illustrated in Fig. 2 where

TABLE II. Convergence of the Hamiltonian for selected vibrational energy levels in the A_1 block using the $F(8)$ basis for the 6th, 10th, 14th orders and for the reduced 14th \rightarrow 6th order. Rms deviations Δ (in cm^{-1}) are given with respect to $H^{(14)}$.

| Band, C | $H^{(6)}$ | $H_{\text{red}}^{(14\rightarrow 6)}$ | $H^{(10)}$ | $H^{(14)}$ | $\Delta H(6)$ | $\Delta H(14 \rightarrow 6)$ | $\Delta H(10)$ |
|--------------|-----------|--------------------------------------|------------|------------|---------------|------------------------------|----------------|
| 001000 A_1 | 1305.71 | 1306.78 | 1306.75 | 1306.80 | 1.09 | 0.03 | 0.06 |
| 010000 A_1 | 2199.43 | 2200.05 | 2199.93 | 2200.01 | 0.58 | −0.04 | 0.08 |
| 000002 A_1 | 2312.62 | 2316.34 | 2315.83 | 2316.22 | 3.61 | −0.12 | 0.40 |
| 002000 A_1 | 2593.56 | 2597.77 | 2597.13 | 2597.57 | 4.01 | −0.20 | 0.44 |
| 000011 A_1 | 2629.77 | 2633.39 | 2632.70 | 2633.24 | 3.47 | −0.15 | 0.54 |
| 000020 A_1 | 2908.32 | 2910.33 | 2909.95 | 2910.21 | 1.89 | −0.12 | 0.25 |
| 100000 A_1 | 2967.12 | 2969.77 | 2969.31 | 2969.74 | 2.62 | −0.03 | 0.43 |
| 000003 A_1 | 3480.93 | 3487.03 | 3486.13 | 3486.89 | 5.96 | −0.15 | 0.75 |
| 011000 A_1 | 3497.49 | 3500.05 | 3499.73 | 3499.99 | 2.50 | −0.05 | 0.26 |
| ... | | | | | | | |
| 001020 A_1 | 4211.07 | 4215.88 | 4215.29 | 4215.88 | 4.80 | 0.00 | 0.59 |
| 101000 A_1 | 4266.84 | 4272.48 | 4271.31 | 4272.36 | 5.52 | −0.13 | 1.04 |
| 020000 A_1 | 4345.26 | 4345.94 | 4345.20 | 4345.32 | 0.07 | −0.61 | 0.12 |
| 000030 A_1 | 4399.81 | 4405.27 | 4403.86 | 4405.09 | 5.28 | −0.19 | 1.23 |
| ... | | | | | | | |
| 010012 A_1 | 5930.20 | 5939.92 | 5937.07 | 5939.31 | 9.11 | −0.62 | 2.24 |
| 000200 A_1 | 5979.68 | 5982.25 | 5981.95 | 5982.05 | 2.37 | −0.20 | 0.10 |

the reduced potential $V_{\text{red}}^{(14\rightarrow 6)}$ allows diminishing the polynomial degree and at the same time pushing away the non-physical feature beyond the dissociation threshold¹⁵ ($D_e(\text{exp}) = 39\,500\text{ cm}^{-1}$). Consequently, the use of $V_{\text{red}}^{(14\rightarrow 6)}$ allows combining the accuracy of $V_{\text{red}}^{(14)}$ at the bottom of the potential well with a better behavior at large nuclear displacements.

Using the basis set (56) and the Wigner-Eckart theorem, the matrix elements are calculated analytically in a very fast way. In Table II, we give the convergence of some selected vibrational energy levels with respect to the Hamiltonian expansions $H^{(6)}$, $H^{(10)}$, $H^{(14)}$, and $H_{\text{red}}^{(14\rightarrow 6)}$ using the $F(8)$ basis. Table II clearly shows that the reduced 14 \rightarrow 6 model is an optimal compromise concerning the ratio *Number of terms/Accuracy*. This procedure introduces very small errors with respect to the full $H^{(14)}$ calculations (see the three last columns of Table II).

• *Basis set compression.* A common challenge in all variational methods for polyatomic molecules is an optimal choice of a limited physically justified subset of vibrational basis functions in order to reduce the cost of calculations. At the same time, one seeks avoiding a loss of accuracy as much as possible. Various techniques of basis truncation-compressions are applied in the literature.^{26,29,52–64,96,97} In order to optimize variational computations of rotation-vibration states, we apply the basis set compression using the vibrational subspace (VSS) approach, which in our implementation can be summarized as follows. Let first solve the pure vibrational stationary Schroedinger equation $H_v \Psi_v = E_v \Psi_v$ using a largest primitive basis set subspace defined by Eq. (57), say $\mathcal{F}(n)$ with $n = v_{\text{max}}$, which is feasible using currently available computational facilities. The resulting anharmonic eigenfunctions are obtained and stored as a combination of uncoupled primitive functions denoted as $\Psi_v^{(n)} = \sum_{\mathcal{F}(n)} c_i \Phi_i$ with the corresponding eigenvalues $E_v^{(n)}$. For example, for purely vibrational part in the case of E block, the number of terms in this expansion for $n = v_{\text{max}} = 10$ in our vibra-

tional calculations was 30 786. This means that in case of vibration-rotation calculations, both the number of basis functions (56) and of terms (43)–(49) in the Hamiltonian rapidly increases resulting in a gigantic set of elementary matrix elements $\langle \Phi_i | V(a^+, a) | \Phi_j \rangle$ to compute. Even though these latter ones are calculated analytically, the rovibrational computations for high J values could become excessively demanding in terms of memory and CPU time. In our VSS approach, we compress the basis set in two steps. As a first step we choose a subspace of primitive functions $\mathcal{F}(r) \subset \mathcal{F}(n)$ corresponding to $v_{\text{max}} = r < n$, for which vibration-rotation calculations are feasible. Then the large basis-set vibrational eigenfunctions $\Psi_v^{(n)} \in \mathcal{F}(n)$ are projected onto the reduced subspace $\mathcal{F}(r)$ and ortho-normalized using a Gram-Schmidt procedure. The resulting set of anharmonic vibrational functions is called *reduced coupled basis set* $\{\Psi_v^{(n\rightarrow r)}\}$. Schematically, we have

$$\mathcal{GP}^{(r)} \Psi_v^{(n)} = \Psi_v^{(n\rightarrow r)} \in \mathcal{F}(r), \quad (58)$$

where $\mathcal{P}^{(r)}$ is a projector onto the $\mathcal{F}(r)$ subspace and \mathcal{G} is the Gram-Schmidt transformation. The second basis compression step is obtained by applying the maximum vibrational energy cutoff $E_v^{(n)} \leq E_{\text{vib}}^{\text{max}}$ to the array $\{E_v^{(n)}, \Psi_v^{(n\rightarrow r)}\}$. The resulting set of vectors is used to build the full rovibrational Hamiltonian matrix by forming the direct product $T = \Psi_v^{(n\rightarrow r)} \otimes \mathbf{I}_{J,C_r}$, where \mathbf{I}_{J,C_r} is the identity matrix in the rotational subspace. The Hamiltonian matrix in the vibrational eigenbasis simply reads

$$\bar{\mathbf{H}} = \mathbf{T}^t \mathbf{H} \mathbf{T} \Rightarrow \mathbf{E}_v \otimes \mathbf{I}_{J,C_r} \delta_{vv'} + \mathbf{H}_{rv}, \quad (59)$$

with

$$\mathbf{H}_{rv} = \mathbf{T}^t \mathbf{h}_{rv} \mathbf{T}, \quad (60)$$

where \mathbf{h}_{rv} is the rovibrational Hamiltonian matrix built in the initial primitive basis set (56). We can then reduce our rovibrational calculations using three cut-off criteria: n and r for

uncoupled subsets and E_{vib}^{max} for the coupled subset. The vibrational energy calculations $E_v^{(n)}$ are ideally converged at $n \rightarrow \infty$ that is not of course directly accessible, but one could replace $E_v^{(n)}$ by E_v^{obs} in Eq. (59) when available. If $E_v^{(n)} \approx E_v^{obs}$ this makes physically meaningful empirical band centers corrections to ro-vibrational variational calculations. In this case both vibrational wave functions $\Psi_v^{(n \rightarrow r)}$ and all ro-vibrational matrix elements H_{rv} in Eq. (59) are still directly computed from *ab initio* PES, but ro-vibrationals eigenvalues and eigenfunctions are better described. This could result then to better predictions of accidental ro-vibrational resonance perturbations in spectra. Alternatively, one could compute better values of $E_v^{(n)}$ using isotopic shifts. The reader can find related illustrations in our previous studies^{29,30} devoted to the tetrahedral methane isotopologues $^{12}\text{CH}_4$, $^{12}\text{CD}_4$, and $^{13}\text{CH}_4$.

As a simple illustration, we have computed the $J = 1$, A_1 rotational energy levels for the bands $\nu_6(E)$, $\nu_2 + \nu_6(E)$, and $\nu_4 + 2\nu_5(A_2)$ centered at 1161, 3342, and 5925 cm^{-1} using the set of eigenvectors $\{\Psi_v^{(6)}, \Psi_v^{(10)}, \Psi_v^{(10 \rightarrow 6)}\}$. For these three bands, the errors $\Delta E = E_{\Psi_v^{(10)}}^{J=1} - E_{\Psi_v^{(6)}}^{J=1}$ are, respectively, $\{0.0005, 0.0018, 0.0306\}$ whereas the errors for the compressed basis $\Delta \tilde{E} = E_{\Psi_v^{(10)}}^{J=1} - E_{\Psi_v^{(10 \rightarrow 6)}}^{J=1}$ are $\{0.0000, 0.0003, 0.0024\}$. We see that $\Psi_v^{(10)}$ and $\Psi_v^{(10 \rightarrow 6)}$ give similar results while the size of the basis is reduced from 45 000 to 2370. In Table III, we give the convergence of the vibrational energy levels as a function of the basis set size. We have considered $F(8)$, $F(9)$, $F(10)$, and $F_\kappa(12)$ primitive basis sets. If all $\kappa_i = 1$, the $F(12)$ basis would require a large amount of memory for storing matrix elements since the size of the E block is $\sim 100\,000$. In what follows, we thus fix $\kappa_4 = 1.05$ with the normal mode quantum number ν_4 belonging to the range $\nu_4 \in \{0, 1, \dots, 11\}$ and $\kappa_i = 1$ for all other modes. This choice is motivated by the fact that the ν_4 mode has the highest frequency and only its second overtone have to be converged up to 8000 cm^{-1} . For each basis, the size N_C of the three blocs $J = 0$ are also specified in this table. CH_3D band centers given in Table IV correspond to our direct variational calculations (TW) from NRT PES without any empirical corrections. In a general manner, our calculations are in very good agreement with experiment. It is also instructive to compare our predictions with the calculations resulting from the effective Hamiltonian (EH) empirical fit of Ref. 50: second column of Table IV. The vibrational shifts $\Delta_v = \text{Obs} - \text{TW}$ we use for the band center corrections $E_v^{(n)} \Rightarrow E_v^{obs}$ in Eq. (59) are those given in the sixth column of Table IV and will be applied in what follows for the VSS procedure. At the next step the primitive $F_\kappa(12)$ basis is used to construct the reduced anharmonic basis functions $\Psi_v^{(12 \rightarrow r)}$ to compute vibration-rotation line positions and intensities.

B. Line strength calculations

The infrared line intensity S_{ij} of a rovibrational transitions ν_{ij} between an initial state i and a final state j for a given temperature T in units [$\text{cm}^{-1}/\text{molecule cm}^{-2}$] is given by

$$S_{ij} = \frac{8\pi^3 10^{-36}}{3hcQ(T)} I_0 g_{C_i} \nu_{ij} e^{-c_2 E_i/T} (1 - e^{-c_2 \nu_{ij}/T}) \times \mathcal{R}_{ij}, \quad (61)$$

where $c_2 = hc/k$, g_{C_i} and E_i are the nuclear spin statistical weight and the energy of the lower state and $Q(T)$ is the partition function. The same units are used in the HITRAN spectroscopic line list compilations. For $^{12}\text{CH}_3\text{D}$ one has $g_{C_i} = 4$ and the partition function taken from HITRAN are $Q = 4774.9815$ at $T = 296$ K. The terrestrial isotopic abundance of $^{12}\text{CH}_3\text{D}$ is $I_0 = 0.000615751$. \mathcal{R}_{ij} corresponds to the square of the transition-moment matrix elements

$$\mathcal{R}_{ij} = \sum_{M_i, M_j} |\langle \Psi_{v_i, M_i, \sigma_i}^{(J_i, C_i)} | \mu_\Theta^s | \Psi_{v_j, M_j, \sigma_j}^{(J_j, C_j)} \rangle|^2, \quad (62)$$

where the summation is over all magnetic sublevels of both initial and final states and Ψ are the eigenfunctions of the ro-vibrational Hamiltonian. In Eq. (62), μ_Θ^s ($\Theta = X, Y, Z$) are the space-fixed electric dipole moment components and are related to molecule-fixed dipole moment components (53) as

$$\mu_Z^s = [\Gamma]^{1/2} \left(C^{(1_s, K, \Gamma)} \otimes \mu^{(\tilde{\Gamma})} \right)^{(A_2)}, \quad (63)$$

where $C_\theta^{(1_s, K, \Gamma)} \equiv \lambda_{Z\theta} \equiv C_{Z\theta}$ are the direction cosines; $\Gamma = A_2, E$ and $\tilde{\Gamma} = A_1, E$. Due to the isotropy of the 3D space, only the Z component is necessary: $\mathcal{R}_{ij} = 3\mathcal{R}_{ij}^Z$.

V. RESULTS: COMPARISONS WITH THE HITRAN 2012 SPECTROSCOPIC DATABASE

There exist several sources of $^{12}\text{CH}_3\text{D}$ data essentially based on raw experimental spectra or line-by-line analyses provided from empirical models.^{39–45,50} Though $^{12}\text{CH}_3\text{D}$ is of major importance in the determination of the H/D ratios in planetary atmospheres, it has been much less studied than the major isotopologue $^{12}\text{CH}_4$. This is partly because its polyad structure is quite different from that of methane leading to various types of the resonance coupling of vibrational subbands in spectra. For $^{12}\text{CH}_4$ there exist a remarkable relation between stretching and bending harmonic frequencies ($\omega_1 \approx \omega_3 \approx 2\omega_2 \approx 2\omega_4$) while a similar relation is only partly valid for $^{12}\text{CH}_3\text{D}$. For instance, by using Eqs. (16)–(18) the polyad number can be expressed as follows:

$$P_{\text{CH}_4} = 2(\omega_1 + \omega_3) + \omega_2 + \omega_4, \quad (64)$$

$$P_{\text{CH}_3\text{D}} \approx 2(\omega_1 + \omega_4) + 1.45\omega_2 + \omega_3 + \omega_5 + 0.8\omega_6.$$

According to the harmonic frequencies given in Table I, the polyads thus cover large spectral ranges and the gaps between them are relatively small compared to methane. The very clear polyad structure of methane CH_4 is broken by the isotopic substitution $H \rightarrow D$ as the frequency of the heavy C–D bond goes down with respect to the light C–H bonds. This leads to an overlapping of “classical” polyads and to a different scheme of resonance couplings. For high energy ranges vibrational levels fill all spectral regions and the definition of polyad is ambiguous. Note that the polyad scheme (64) is well adapted for building so-called effective Hamiltonians. However, it was shown in Table V of Ref. 67 that the

TABLE III. Comparison of CH₃D vibration level calculations for various basis sets. (a) Zero point energy values (in cm⁻¹) and basis size. (b) Convergence of the vibrational energy levels (in cm⁻¹) using the Hamiltonian reduction model $H_{\text{red}}^{14 \rightarrow 6}$ and the $F(8)$, $F(9)$, $F(10)$, and $F_{\kappa}(12)$ ($\kappa_4 = 1.05$) basis sets.

| (a) | | | | | | | |
|--------------|----------|----------|----------|------------------|--------------------|------------------|-------------------|
| Block | $F(8)$ | $F(9)$ | $F(10)$ | $F_{\kappa}(12)$ | | | |
| N_{A_1} | 4426 | 8698 | 16306 | 32737 | | | |
| N_{A_2} | 3684 | 7522 | 14500 | 29461 | | | |
| N_E | 8100 | 16200 | 30786 | 62163 | | | |
| ZPE | 9078.436 | 9078.431 | 9078.430 | 9078.430 | | | |
| (b) | | | | | | | |
| Band, C | $F(8)$ | $F(9)$ | $F(10)$ | $F_{\kappa}(12)$ | $\Delta F(12-8)^a$ | $\Delta F(12-9)$ | $\Delta F(12-10)$ |
| 000001 E | 1161.02 | 1161.02 | 1161.01 | 1161.01 | -0.01 | -0.01 | 0 |
| 001000 A_1 | 1306.78 | 1306.78 | 1306.77 | 1306.77 | -0.01 | -0.01 | 0 |
| 000010 E | 1472.03 | 1472.03 | 1472.03 | 1472.02 | -0.01 | -0.01 | -0.01 |
| 010000 A_1 | 2200.05 | 2200.02 | 2200.01 | 2200.01 | -0.04 | -0.01 | 0 |
| 000002 A_1 | 2316.34 | 2316.24 | 2316.23 | 2316.22 | -0.12 | -0.02 | -0.01 |
| 000002 E | 2323.27 | 2323.18 | 2323.17 | 2323.16 | -0.11 | -0.02 | -0.01 |
| 001001 E | 2465.62 | 2465.51 | 2465.50 | 2465.49 | -0.13 | -0.02 | -0.01 |
| 002000 A_1 | 2597.77 | 2597.65 | 2597.63 | 2597.62 | -0.15 | -0.03 | -0.01 |
| 000011 E | 2623.55 | 2623.46 | 2623.45 | 2623.44 | -0.11 | -0.02 | -0.01 |
| 000011 A_1 | 2633.39 | 2633.30 | 2633.28 | 2633.28 | -0.11 | -0.02 | 0 |
| 000011 A_2 | 2634.98 | 2634.88 | 2634.87 | 2634.87 | -0.11 | -0.01 | 0 |
| 001010 E | 2776.52 | 2776.42 | 2776.41 | 2776.40 | -0.12 | -0.02 | -0.01 |
| 000020 A_1 | 2910.33 | 2910.26 | 2910.25 | 2910.24 | -0.09 | -0.02 | -0.01 |
| 000020 E | 2940.31 | 2940.22 | 2940.21 | 2940.20 | -0.11 | -0.02 | -0.01 |
| 100000 A_1 | 2969.77 | 2969.68 | 2969.66 | 2969.65 | -0.12 | -0.03 | -0.01 |
| 000100 E | 3016.78 | 3016.72 | 3016.70 | 3016.69 | -0.09 | -0.03 | -0.01 |
| 010001 E | 3342.63 | 3342.38 | 3342.34 | 3342.32 | -0.31 | -0.06 | -0.02 |
| 000003 E | 3472.24 | 3471.64 | 3471.50 | 3471.47 | -0.77 | -0.17 | -0.03 |
| 000003 A_1 | 3487.03 | 3486.42 | 3486.30 | 3486.28 | -0.75 | -0.14 | -0.02 |
| 000003 A_2 | 3487.38 | 3486.78 | 3486.66 | 3486.64 | -0.74 | -0.14 | -0.02 |
| 011000 A_1 | 3500.05 | 3499.77 | 3499.72 | 3499.70 | -0.35 | -0.07 | -0.02 |
| ... | | | | | | | |
| 000101 A_2 | 4175.45 | 4175.02 | 4174.95 | 4174.92 | -0.53 | -0.1 | -0.03 |
| 001020 A_1 | 4215.88 | 4215.44 | 4215.35 | 4215.32 | -0.56 | -0.12 | -0.03 |
| 001020 E | 4242.82 | 4242.31 | 4242.18 | 4242.16 | -0.66 | -0.15 | -0.02 |
| 101000 A_1 | 4272.48 | 4271.92 | 4271.80 | 4271.76 | -0.72 | -0.16 | -0.04 |
| 001100 E | 4313.52 | 4313.05 | 4312.97 | 4312.94 | -0.58 | -0.11 | -0.03 |
| 020000 A_1 | 4345.93 | 4344.79 | 4344.56 | 4344.45 | -1.48 | -0.34 | -0.11 |
| 100010 E | 4357.44 | 4357.06 | 4356.98 | 4356.95 | -0.49 | -0.11 | -0.03 |
| 000030 A_2 | 4403.60 | 4403.11 | 4403.00 | 4402.98 | -0.62 | -0.13 | -0.02 |
| 000030 A_1 | 4405.27 | 4404.77 | 4404.66 | 4404.64 | -0.63 | -0.13 | -0.02 |
| 000030 E | 4440.80 | 4440.22 | 4440.09 | 4440.06 | -0.74 | -0.16 | -0.03 |
| ... | | | | | | | |
| 010012 A_2 | 5937.87 | 5935.86 | 5934.66 | 5934.30 | -3.57 | -1.56 | -0.36 |
| 010012 E | 5939.81 | 5936.75 | 5935.43 | 5934.96 | -4.85 | -1.79 | -0.47 |
| 010012 A_1 | 5939.92 | 5937.84 | 5936.66 | 5936.29 | -3.63 | -1.55 | -0.37 |
| 001004 E | 5952.67 | 5947.84 | 5946.31 | 5945.63 | -7.04 | -2.21 | -0.68 |
| 010012 E | 5965.32 | 5962.28 | 5961.13 | 5960.67 | -4.65 | -1.61 | -0.46 |
| 000200 A_1 | 5982.25 | 5980.90 | 5980.55 | 5980.44 | -1.81 | -0.46 | -0.11 |

^a $\Delta F(12 - k)$ is the discrepancy (in cm⁻¹) of calculated levels using $F(12)$ and $F(k)$ basis sets.

$F_{\kappa}(v_{\text{max}})$ pruning scheme allows more flexible optimization of variational calculations. Moreover, the symmetry is lower and as a direct consequence some degeneracies are removed due to the isotopic substitution (see Eqs. (A1) and (A3), for instance) and the number of levels in the harmonic approximation is larger. The first interacting band system is the Triad (ν_3, ν_5, ν_6) which corresponds to the Dyad of methane while

the next one called Nonad ($\nu_1, \nu_2, \nu_3, 2\nu_3, 2\nu_5, 2\nu_6, \nu_3 + \nu_5, \nu_3 + \nu_6, \nu_5 + \nu_6$) corresponds to the methane Pentad. The current analyses⁴⁵ of ¹²CH₃D are focusing on the so-called Enneadecad region involving 19 interacting states and some additional ones, which roughly speaking could be considered as a counterpart of the Octad (2.1–2.8 μm) for ¹²CH₄. However, it turns out that some additional bands coming from the

TABLE IV. Comparison of variational predictions for $^{12}\text{CH}_3\text{D}$ band centers (TW) with vibrational levels deduced from experimental spectra and with effective Hamiltonian (EH) fits. Selected vibrational band centers of $^{12}\text{CH}_3\text{D}$ computed variationally with the $F_\kappa(12)$ ($\kappa_4 = 1.05$) basis and using the ITO normal mode Hamiltonian reduction model $H_{\text{red}}^{(14 \rightarrow 6)}$ (This Work, TW), compared to experimental values^{41,42,44,45,50} and to those of Ref. 50 obtained from an empirical model. (Note: TW (this work), computed from NRT methane PES. Obs: experimentally deduced values,^{41,42,44,45,50} EH: (Calc. II, Table 12 of Ref. 50) calculations using effective Hamiltonian empirical fit. All values are in cm^{-1} .)

| Band, Sym | EH. ⁵⁰ | TW | Obs. | TW-EH. ⁵⁰ | Obs.-TW | Obs.-EH. ⁵⁰ |
|-----------------------------|-------------------|---------|---------|----------------------|---------|------------------------|
| $\nu_6 E$ | 1160.74 | 1161.01 | 1161.10 | 0.27 | 0.09 | 0.36 |
| $\nu_3 A_1$ | 1307.48 | 1306.77 | 1306.85 | -0.71 | 0.08 | -0.63 |
| $\nu_5 E$ | 1472.16 | 1472.02 | 1472.02 | -0.14 | 0.00 | -0.14 |
| $\nu_2 A_1$ | 2199.08 | 2200.01 | 2200.04 | 0.93 | 0.03 | 0.96 |
| $2\nu_6 A_1$ | 2316.37 | 2316.22 | 2316.27 | -0.15 | 0.06 | -0.10 |
| $2\nu_6 E$ | 2322.44 | 2323.16 | 2323.29 | 0.72 | 0.13 | 0.85 |
| $\nu_3 + \nu_6 E$ | 2465.14 | 2465.49 | 2465.46 | 0.35 | -0.03 | 0.32 |
| $2\nu_3 A_1$ | 2598.57 | 2597.62 | 2597.69 | -0.95 | 0.06 | -0.88 |
| $\nu_5 + \nu_6 E$ | 2623.13 | 2623.44 | 2623.44 | 0.31 | 0.00 | 0.31 |
| $\nu_5 + \nu_6 A_1$ | 2633.37 | 2633.28 | 2633.16 | -0.09 | -0.12 | -0.21 |
| $\nu_5 + \nu_6 A_2$ | | 2634.87 | 2634.84 | | -0.03 | |
| $\nu_3 + \nu_5 E$ | 2776.73 | 2776.40 | 2776.29 | -0.33 | -0.11 | -0.44 |
| $2\nu_5 A_1$ | 2910.01 | 2910.24 | 2910.12 | 0.23 | -0.12 | 0.10 |
| $2\nu_5 E$ | 2940.25 | 2940.20 | 2940.10 | -0.05 | -0.10 | -0.15 |
| $\nu_1 A_1$ | 2969.49 | 2969.65 | 2969.51 | 0.16 | -0.14 | 0.02 |
| $\nu_4 E$ | 3015.90 | 3016.69 | 3016.71 | 0.79 | 0.02 | 0.81 |
| $\nu_2 + \nu_6 E$ | 3342.24 | 3342.32 | 3342.57 | 0.08 | 0.25 | 0.33 |
| $3\nu_6 E$ | 3471.66 | 3471.47 | 3471.47 | -0.19 | -0.01 | -0.19 |
| $3\nu_6 A_1$ | 3483.79 | 3486.28 | 3486.45 | 2.49 | 0.18 | 2.66 |
| $3\nu_6 A_2$ | | 3486.64 | 3486.72 | | 0.08 | |
| $\nu_2 + \nu_3 A_1$ | 3499.25 | 3499.70 | 3499.72 | 0.45 | 0.02 | 0.47 |
| $\nu_3 + 2\nu_6 A_1$ | 3617.71 | 3617.19 | 3616.80 | -0.52 | -0.39 | -0.91 |
| $\nu_3 + 2\nu_6 E$ | 3623.77 | 3625.26 | 3625.01 | 1.49 | -0.25 | 1.24 |
| $\nu_2 + \nu_5 E$ | 3667.72 | 3668.07 | 3668.08 | 0.35 | 0.00 | 0.36 |
| $2\nu_3 + \nu_6 E$ | 3752.74 | 3754.19 | 3753.88 | 1.45 | -0.30 | 1.14 |
| $\nu_5 + 2\nu_6 A_2$ | | 3775.36 | | | | |
| $\nu_5 + 2\nu_6 A_1$ | 3775.05 | 3776.58 | | 1.52 | | |
| $\nu_5 + 2\nu_6 1E$ | 3778.91 | 3780.01 | 3779.76 | 1.10 | -0.25 | 0.85 |
| $\nu_5 + 2\nu_6 2E$ | 3794.53 | 3797.26 | | 2.72 | | |
| $3\nu_3 A_1$ | 3874.39 | 3874.86 | 3874.74 | 0.47 | -0.12 | 0.35 |
| $\nu_3 + \nu_5 + \nu_6 E$ | 3924.62 | 3925.58 | 3925.20 | 0.96 | -0.38 | 0.58 |
| $\nu_3 + \nu_5 + \nu_6 A_1$ | 3935.48 | 3935.69 | 3935.25 | 0.21 | -0.44 | -0.23 |
| $\nu_3 + \nu_5 + \nu_6 A_2$ | | 3936.70 | 3936.27 | | -0.44 | |
| $2\nu_5 + \nu_6 1E$ | 4059.68 | 4058.88 | 4058.69 | -0.80 | -0.19 | -0.99 |
| $2\nu_3 + \nu_5 E$ | 4066.73 | 4067.99 | 4067.85 | 1.26 | -0.14 | 1.12 |
| $2\nu_5 + \nu_6 A_1$ | 4081.44 | 4081.59 | 4081.33 | 0.14 | -0.25 | -0.11 |
| $2\nu_5 + \nu_6 A_2$ | | 4082.88 | | | | |
| $2\nu_5 + \nu_6 2E$ | 4101.02 | 4102.81 | 4102.44 | 1.79 | -0.37 | 1.42 |
| $\nu_1 + \nu_6 E$ | 4122.10 | 4122.72 | 4122.59 | 0.62 | -0.13 | 0.49 |
| $\nu_4 + \nu_6 A_1$ | 4164.18 | 4163.18 | 4163.49 | -1.00 | 0.31 | -0.69 |
| $\nu_4 + \nu_6 E$ | 4170.50 | 4170.08 | | -0.42 | | |
| $\nu_4 + \nu_6 A_2$ | | 4174.92 | | | | |
| $\nu_3 + 2\nu_5 A_1$ | 4214.98 | 4215.32 | 4215.29 | 0.34 | -0.03 | 0.31 |
| $\nu_3 + 2\nu_5 E$ | 4241.92 | 4242.16 | 4241.74 | 0.24 | -0.42 | -0.18 |
| $\nu_3 + \nu_4 E$ | 4312.86 | 4312.94 | 4313.42 | 0.08 | 0.49 | 0.56 |
| $2\nu_2 A_1$ | 4342.27 | 4344.45 | 4344.12 | 2.18 | -0.32 | 1.85 |
| $3\nu_5 E$ | 4356.27 | 4356.96 | 4356.89 | 0.68 | -0.07 | 0.62 |
| $3\nu_5 A_2$ | | 4402.98 | | | | |
| $3\nu_5 A_1$ | 4404.27 | 4404.64 | 4404.36 | 0.37 | -0.28 | 0.09 |
| $\nu_1 + \nu_5 E$ | 4440.71 | 4440.06 | 4439.73 | -0.65 | -0.33 | -0.98 |
| $\nu_4 + \nu_5 A_2$ | | 4471.41 | | | | |
| $\nu_4 + \nu_5 E$ | 4472.63 | 4472.42 | 4472.65 | -0.22 | 0.23 | 0.02 |
| $\nu_2 + 2\nu_6 A_1$ | 4486.76 | 4484.82 | 4484.82 | -1.94 | 0.00 | -1.94 |
| $\nu_4 + \nu_5 E$ | 4486.34 | 4486.73 | 4486.88 | 0.39 | 0.15 | 0.54 |
| $4\nu_6 A_1$ | 4619.24 | 4618.71 | 4618.45 | -0.53 | -0.26 | -0.79 |

TABLE IV. (Continued.)

| Band, Sym | EH. ⁵⁰ | TW | Obs. | TW-EH. ⁵⁰ | Obs.-TW | Obs.-EH. ⁵⁰ |
|--------------------------------|-------------------|---------|---------|----------------------|---------|------------------------|
| $4\nu_6$ $1E$ | 4625.31 | 4627.07 | 4626.92 | 1.76 | −0.15 | 1.61 |
| $\nu_2 + \nu_3 + \nu_6$ E | 4639.33 | 4639.86 | | 0.52 | | |
| $\nu_3 + 3\nu_6$ E | 4769.92 | 4769.42 | | −0.50 | | |
| $\nu_3 + 3\nu_6$ A_1 | 4782.83 | 4781.54 | 4781.53 | −0.50 | 0.02 | −1.27 |
| $\nu_3 + 3\nu_6$ A_2 | | 4785.95 | | | | |
| $\nu_2 + 2\nu_3$ A_1 | 4782.04 | 4786.73 | | 4.69 | | |
| $\nu_2 + \nu_5 + \nu_6$ E | 4801.10 | 4800.53 | | −0.57 | | |
| $\nu_2 + \nu_5 + \nu_6$ A_1 | 4811.54 | 4811.24 | 4811.17 | −0.30 | −0.07 | −0.37 |
| $\nu_2 + \nu_5 + \nu_6$ A_2 | | 4812.72 | | | | |
| $2\nu_3 + 2\nu_6$ A_1 | 4901.65 | 4903.18 | 4901.42 | 1.53 | −1.76 | −0.23 |
| $2\nu_3 + 2\nu_6$ E | 4907.72 | 4912.03 | | 4.31 | | |
| $\nu_5 + 3\nu_6$ $1E$ | 4924.76 | 4925.93 | | 1.17 | | |
| $\nu_5 + 3\nu_6$ $2E$ | 4926.63 | 4929.96 | | 3.33 | | |
| $\nu_5 + 3\nu_6$ A_1 | 4935.11 | 4935.20 | 4934.51 | 0.09 | −0.69 | −0.60 |
| $\nu_5 + 3\nu_6$ A_2 | | 4938.34 | | | | |
| $\nu_5 + 3\nu_6$ $3E$ | 4955.70 | 4961.53 | | 5.83 | | |
| $\nu_2 + \nu_3 + \nu_5$ E | 4964.98 | 4965.49 | | 0.51 | | |
| $3\nu_3 + \nu_6$ E | 5027.40 | 5030.33 | | 2.93 | | |
| $\nu_3 + \nu_5 + 2\nu_6$ A_2 | | 5075.53 | | | | |
| $\nu_3 + \nu_5 + 2\nu_6$ A_1 | 5073.48 | 5076.29 | | 2.81 | | |
| $\nu_3 + \nu_5 + 2\nu_6$ $1E$ | 5077.57 | 5079.02 | | 1.45 | | |
| $\nu_3 + \nu_5 + 2\nu_6$ $2E$ | 5093.61 | 5096.86 | | 3.25 | | |
| $\nu_2 + 2\nu_5$ A_1 | 5103.53 | 5103.71 | 5103.57 | 0.18 | −0.14 | 0.04 |
| $\nu_2 + 2\nu_5$ E | 5132.29 | 5132.26 | 5132.10 | −0.03 | −0.15 | −0.19 |
| $4\nu_3$ A_1 | 5134.70 | 5139.32 | | 4.62 | | |
| $\nu_1 + \nu_2$ A_1 | 5164.53 | 5165.19 | 5165.05 | 0.66 | −0.15 | 0.52 |
| $2\nu_3 + \nu_5 + \nu_6$ E | 5206.68 | 5207.25 | | 0.57 | | |
| $2\nu_5 + 2\nu_6$ $1A_1$ | 5206.55 | 5209.05 | | 2.50 | | |
| rms | | | | 1.69 | 0.33 | 0.88 |

Tetradecad of methane have to be included in the Enneadecad to take into account more resonance terms in effective Hamiltonian models. This issue will be discussed in a forthcoming paper. For this work, the major advantage of global variational calculations combined with a symmetry-adapted model is that all interacting terms are inherently considered. They are essential to correctly model intensity transfers due to accidental resonances. For the calculation of the energy levels, we proceed exactly in the same manner as for our previous works on methane. As the size the basis set rapidly increases with J , the rovibrational problem is partitioned into three parts. Starting from the reduction of $J = 0$ eigenfunctions $\Psi_v^{(12 \rightarrow r)}$, the rovibrational calculations were carried out with $r = 7$ for $1 \leq J \leq 6$, with $r = 6$ for $7 \leq J \leq 15$ and with $r = 5$ for $16 \leq J \leq 15$. The vibrational energy cut-off energy E_{vib}^{max} was applied to choose approximately 80% of the eigenvectors during the VSS process. This corresponds to $E_{vib}^{max} = 12\,400\text{ cm}^{-1}$, $10\,750\text{ cm}^{-1}$, and $9\,200\text{ cm}^{-1}$ for these three ranges of quantum numbers. The largest bloc to be diagonalized in this work corresponds to $(J, C) = (15, E)$ with the $(12 \rightarrow 6)$ eigenfunction reduction. Its size is 51 715 that reduced to 41 042 when applying the VSS procedure.

To validate our results both for positions and intensities, all present calculations were compared to the last release of HITRAN2012 database⁴⁶ at $T = 296\text{ K}$. This HITRAN list is

essentially a compilation of lines which come from (i) spectroscopic analyses using empirically-fitted effective models ($<4500\text{ cm}^{-1}$) and (ii) the WKL^{MC}⁴⁹ experimental line list ($>6000\text{ cm}^{-1}$). In the first case, the included lines are fully

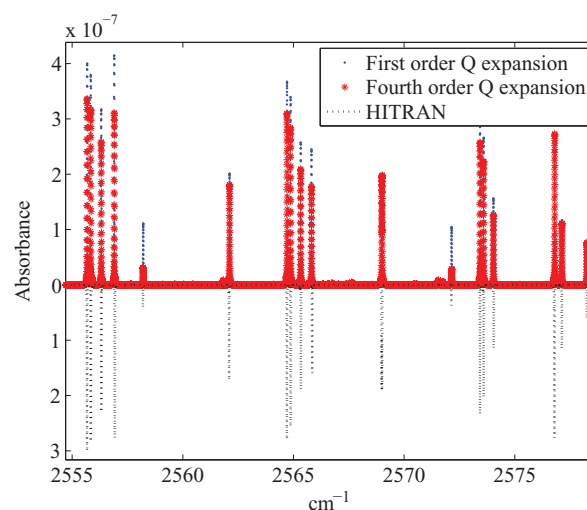


FIG. 3. Convergence of calculated line intensities of $^{12}\text{CH}_3\text{D}$ (positive axis) in the $2\nu_3(A_1)$ region with respect to the order of the power series (35) in comparison with HITRAN 2012.⁴⁶ The first order expansion corresponds to the rectilinear approximation (15).

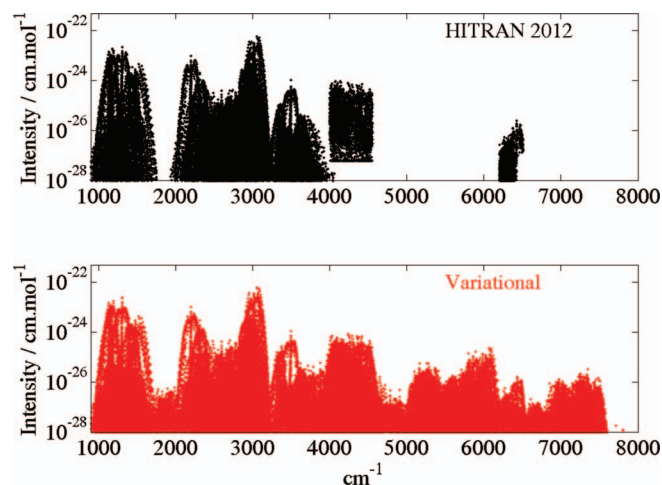


FIG. 4. Overview spectrum of $^{12}\text{CH}_3\text{D}$ from 0 to 8000 cm^{-1} . Comparison between first principles calculations (this work) and the HITRAN 2012 empirical database at $T = 296\text{ K}$ in log scale. The theoretical line list contains over 2 000 000 transitions with $J_{\text{max}} = 25$ up to a lower state energy E_{low} of 4000 cm^{-1} and with a intensity cutoff of $I_0 \times 10^{-27}\text{ cm/mol}$. HITRAN 2012 contains 50 550 lines.

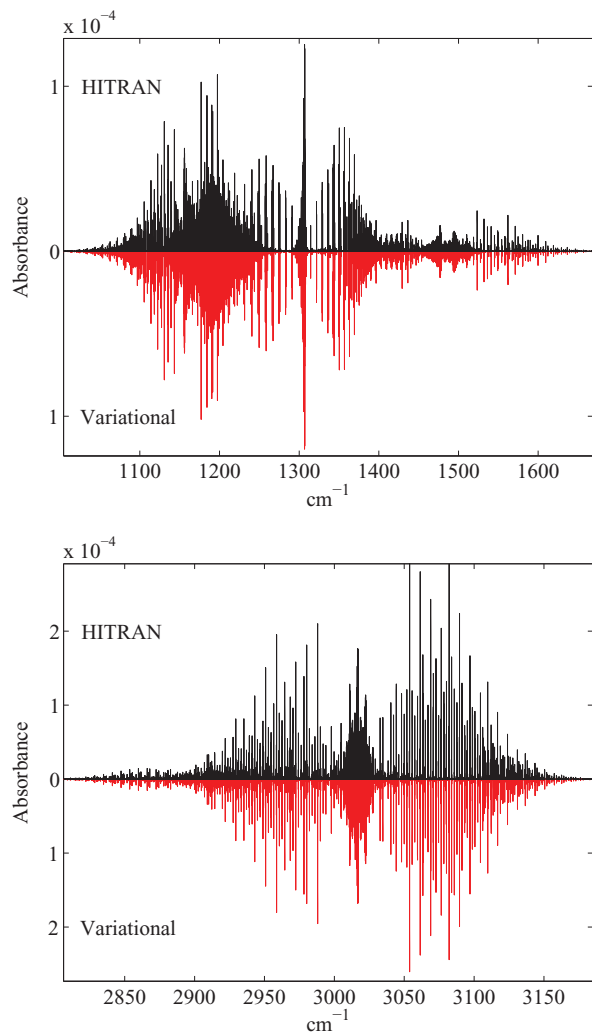


FIG. 5. Comparison of the $^{12}\text{CH}_3\text{D}$ spectrum in the triad (upper panel) and nonad (lower panel) regions between variational calculations and HITRAN 2012 at $T = 296\text{ K}$. The spectra were computed with a line profile at a resolution of 0.001 cm^{-1} and band centers were shifted in the VSS procedure by Δ_v (see column 6 of Table IV).

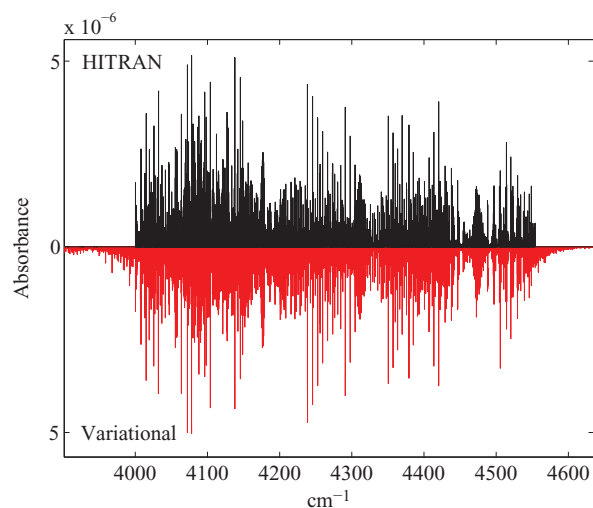


FIG. 6. Comparison of the spectrum in the third polyad region of $^{12}\text{CH}_3\text{D}$ between variational calculations and HITRAN 2012 at $T = 296\text{ K}$. The spectra were computed with a line profile at a resolution of 0.001 cm^{-1} and band centers were shifted in the VSS procedure by Δ_v (see column 6 of Table IV).

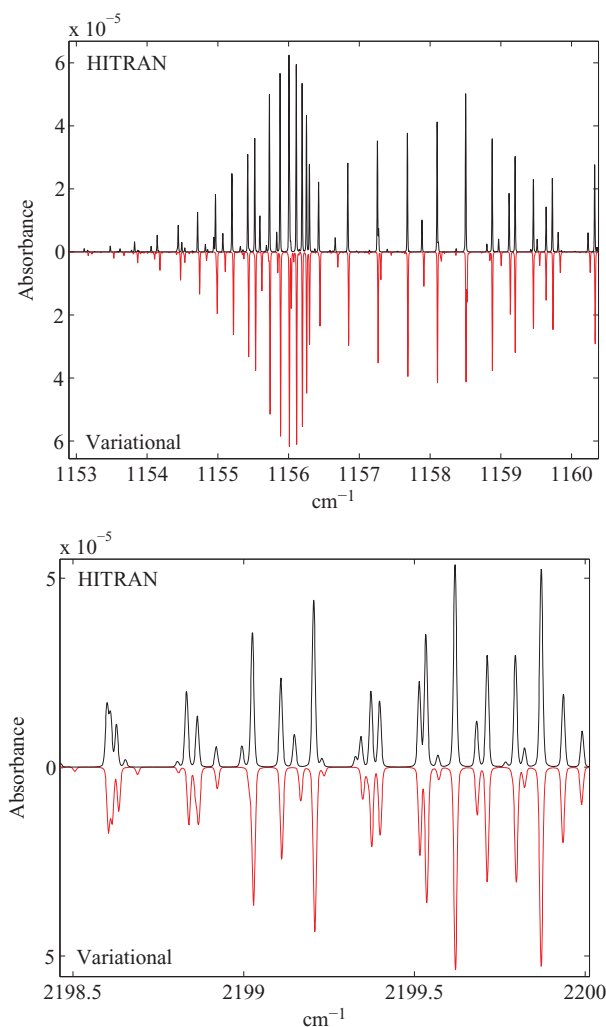


FIG. 7. Comparison for detailed portions of the absorption spectra of $^{12}\text{CH}_3\text{D}$ between variational using *ab initio* DMS and HITRAN 2012 at $T = 296\text{ K}$. Spectra simulations use line profile at a resolution of 0.001 cm^{-1} .

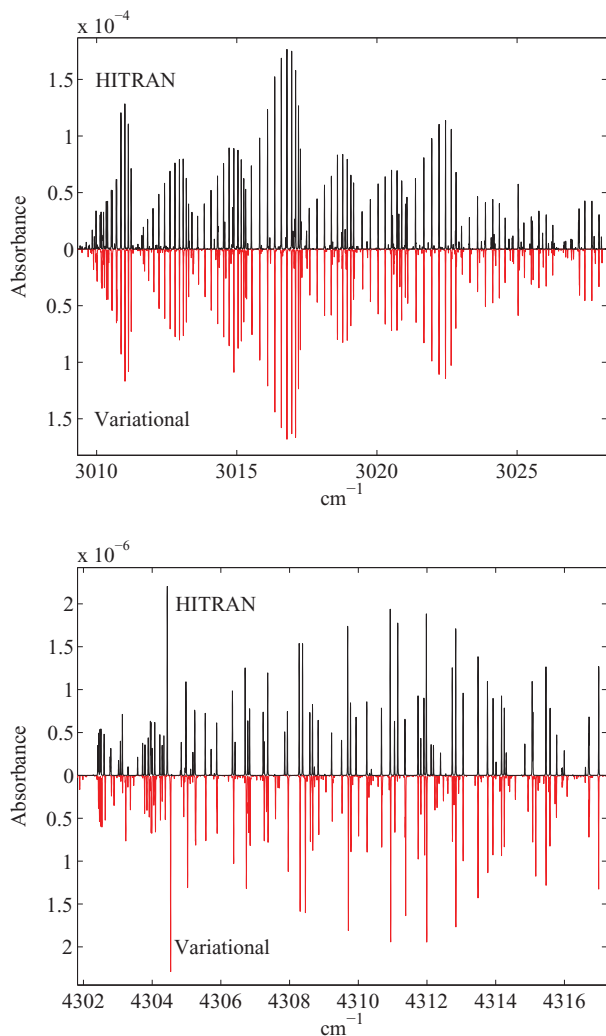


FIG. 8. Comparison for detailed portions of the absorption spectra of $^{12}\text{CH}_3\text{D}$ between variational using *ab initio* DMS and HITRAN 2012 at $T = 296$ K. Spectra simulations use line profile at a resolution of 0.001 cm^{-1} .

assigned. In the second case, only some lower state energies obtained from the two-temperature method relying on an extraction of the Boltzmann factor from measured line strengths have been provided. Before making direct comparisons we have first studied the convergence of line intensities with respect to the truncation order of the power series (35). This latter expansion is used for converting the T_d methane dipole moment expansion (50) into forms (52) and (53) adapted to $^{12}\text{CH}_3\text{D}$. The convergence is well illustrated by Fig. 3 in the $2\nu_3(A_1)$ region where the first order rectilinear approximation in normal coordinate transformations, Eq. (35), and the fourth order one are considered. We clearly see that keeping only linear terms in Eq. (35) is not sufficient to obtain accurate results in this region while the fourth order expansion gives a good agreement. In a general manner our calculations suggested that the second order expansion in (35) was sufficient and gave results similar to that obtained from order 4, at least for the spectral range considered in this work and for medium and strong lines. But to keep security margins in our calculations, the power series (35) was truncated at the fourth order in q transforma-

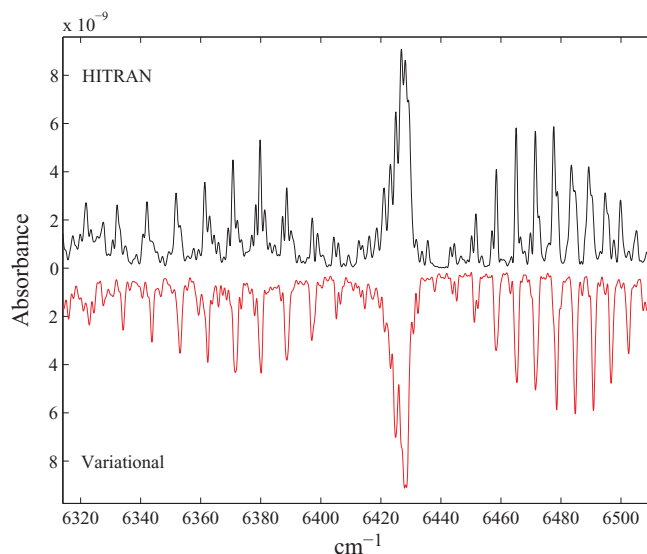


FIG. 9. Comparison of detailed portions of the absorption spectra in the region of $3\nu_2$ between variational calculations using *ab initio* DMS and HITRAN 2012 at $T = 296$ K. Spectra simulations use line profile at the resolution of 0.1 cm^{-1} . The band center was shifted to that of Ref. 50.

tions during this work. Fig. 4 gives a bird's-eyes overview of the absorption $^{12}\text{CH}_3\text{D}$ spectra up to 8000 cm^{-1} in log scale. It shows a very good qualitative agreement between our variational calculations and HITRAN2012⁴⁶ for the subset of lines present both in theoretical and in empirically-derived lists. It is seen that our list contains much more information above 4500 cm^{-1} . This missing information is expected to be crucial for the quantitative modeling of various planetary atmospheres. Our final room-temperature line list in the range $[0-8000]\text{ cm}^{-1}$ contains over 2×10^6 lines calculated at $J_{\max} = 25$ up to a lower state energy E_{low} of 4000 cm^{-1} and with a intensity cutoff of $I_0 \times 10^{-27}\text{ cm/mol}$. Up to the Enneadecad region ($<5000\text{ cm}^{-1}$), our list contains 987 000 lines composed of 272 000 cold band and 715 000 hot band transitions, for this latter case essentially for Triad-Triad and Nonad-Triad-type transitions. Figs. 5–8 show an absorption spectra in comparison with HITRAN in the Triad, Nonad, and Enneadecad regions while Fig. 9 gives a comparison of low resolution spectra in the $3\nu_2$ region. In particular, Fig. 6 shows that the HITRAN database is not complete and that much more line-by-line analyses are necessary to fill empty regions. We hope that this work would help resolving this issue by providing a complete set of missing information for room- and cold-T conditions. The complete line list of $^{12}\text{CH}_3\text{D}$ up to 5000 cm^{-1} with a intensity cutoff of $I_0 \times 10^{-25}\text{ cm/mol}$ and composed of $\sim 180\text{ 000}$ transitions is provided in the supplementary materials.⁸⁷

VI. CONCLUSION

In this work we have presented global calculations for $^{12}\text{CH}_3\text{D}$ based on (i) accurate *ab initio* calculations, (ii) symmetry and coordinate transformations, and (iii) a systematic theoretical procedure for solving the nuclear motion problem. For the very first time for a penta-atomic

symmetric-top molecule, *ab initio* predictions are in excellent quantitative agreement with the HITRAN database in the range corresponding to line-by-line analyses. Moreover global predictions can provide complementary information to existing databases in the regions above 4500 cm⁻¹ where few studies exist. This could certainly help resolving many issues related to assignments of observed spectra. To conclude, this work is a big step forward to build future low, medium, and hot temperature synthetic line lists which will be important for modelling, for example, the Titan's atmosphere or the opacity in atmospheres of exoplanets.

ACKNOWLEDGMENTS

Support for this work was provided by IDRIS computer centre of CNRS, CINES computer centre of France as well as the Romeo computer centre Reims-Champagne-Ardenne. This work has been partly supported by French-Russian collaboration project SAMIA, by the methane project of French "Programme National de la Planetologie," by visiting program of Reims University as well as by Tomsk State University Competitiveness Improvement Program.

APPENDIX: $T_d \leftrightarrow C_{3v}$ AXIS SWITCHING FOR CH₄

Although it may not seem natural it is technically convenient to treat XY₄ molecules as C_{3v} species. In that case we do not keep advantage of the full symmetry but this allows to consider a unified treatment of both XY₄ and XY₃Z-type molecules in relation with isotopic substitutions. As stated in Sec. II the passage from T_d to C_{3v} is not direct because of different conventions for the molecular axis system. For T_d the quantization axis (Oz) is taken as one of the S_4 axes while for C_{3v} the (Oz) axis coincides with the C_3 axis along the $X - Z$ bond (where the XY₃ group rotates). This transformation is thus carried out by two successive rotations, explicitly expressed by the rotation matrix $R(\Omega) = R(\frac{\pi}{4}, \cos^{-1}\frac{1}{\sqrt{3}}, 0)$ in Eqs. (8)–(68a) of Ref. 98. Consequently, we can link together the molecular frame components of the total angular momentum by

$$\begin{pmatrix} J_x^{(F_1)} \\ J_y^{(F_1)} \\ J_z^{(F_1)} \end{pmatrix}_{T_d} = \mathcal{R}_J \begin{pmatrix} J_{y,a}^{(E)} \\ J_{x,b}^{(E)} \\ J_z^{(A_2)} \end{pmatrix}_{C_{3v}}, \quad (\text{A1})$$

where

$$\mathcal{R}_J = \begin{pmatrix} \frac{1}{\sqrt{2}} & -\frac{1}{\sqrt{6}} & \frac{1}{\sqrt{3}} \\ -\frac{1}{\sqrt{2}} & -\frac{1}{\sqrt{6}} & \frac{1}{\sqrt{3}} \\ 0 & \frac{2}{\sqrt{6}} & \frac{1}{\sqrt{3}} \end{pmatrix}. \quad (\text{A2})$$

The symmetry coordinates are also transformed as $\mathbf{S}^{T_d} = \mathcal{U} \mathbf{S}^{C_{3v}}$ or more explicitly as

$$\begin{pmatrix} S_1^{(A_1)} \\ S_{2a}^{(E)} \\ S_{2b}^{(E)} \\ S_{3x}^{(F_2)} \\ S_{3y}^{(F_2)} \\ S_{3z}^{(F_2)} \\ S_{4x}^{(F_2)} \\ S_{4y}^{(F_2)} \\ S_{4z}^{(F_2)} \end{pmatrix}_{T_d} = \mathcal{U}_S \begin{pmatrix} S_1^{(A_1)} \\ S_2^{(A_1)} \\ S_3^{(A_1)} \\ S_{4a}^{(E)} \\ S_{4b}^{(E)} \\ S_{5a}^{(E)} \\ S_{5b}^{(E)} \\ S_{6a}^{(E)} \\ S_{6b}^{(E)} \end{pmatrix}_{C_{3v}} \quad (\text{A3})$$

with

$$\mathcal{U}_S = \begin{pmatrix} \frac{\sqrt{3}}{2} & 0 & \frac{1}{2} & 0 & 0 & 0 & 0 & 0 & 0 \\ 0 & 0 & 0 & 0 & 0 & 0 & 0 & 1 & 0 \\ 0 & 0 & 0 & 0 & 0 & 0 & 0 & 0 & 1 \\ -\frac{\sqrt{3}}{6} & 0 & \frac{1}{2} & \frac{1}{\sqrt{6}} & -\frac{1}{\sqrt{2}} & 0 & 0 & 0 & 0 \\ -\frac{\sqrt{3}}{6} & 0 & \frac{1}{2} & \frac{1}{\sqrt{6}} & \frac{1}{\sqrt{2}} & 0 & 0 & 0 & 0 \\ -\frac{\sqrt{3}}{6} & 0 & \frac{1}{2} & -\frac{2}{\sqrt{6}} & 0 & 0 & 0 & 0 & 0 \\ 0 & \frac{1}{\sqrt{3}} & 0 & 0 & 0 & -\frac{1}{\sqrt{6}} & \frac{1}{\sqrt{2}} & 0 & 0 \\ 0 & \frac{1}{\sqrt{3}} & 0 & 0 & 0 & -\frac{1}{\sqrt{6}} & -\frac{1}{\sqrt{2}} & 0 & 0 \\ 0 & \frac{1}{\sqrt{3}} & 0 & 0 & 0 & \frac{2}{\sqrt{6}} & 0 & 0 & 0 \end{pmatrix}. \quad (\text{A4})$$

So the PES for methane can be expressed in terms of C_{3v} symmetry coordinates when dealing with XY₃Z isotopologues. According to the relation (13) we can also derive a very useful relation,

$$\mathbf{X}^{T_d} = (\mathbf{L}_q^{T_d})^{-1} \mathcal{U}_S \mathbf{L}_q^{C_{3v}} \mathbf{X}^{C_{3v}} \equiv \mathcal{U}_q \mathbf{X}^{C_{3v}}, \quad (\text{A5})$$

where \mathbf{X} can be, for example, the vectors \mathbf{q} , \mathbf{a} or \mathbf{a}^+ . The " q " index means that we work with dimensionless coordinates that is $[\mathbf{S}^{(\Gamma)}]_{\text{rect}} = \mathbf{L}_q \mathbf{q}^{(\Gamma)}$. As a simple application, for XY₄

molecules we have the following $T_d \rightarrow C_{3v}$ transformation:

$$U_q = \begin{pmatrix} 0 & 1 & 0 & 0 & 0 & 0 & 0 & 0 & 0 \\ 0 & 0 & 0 & 0 & 0 & 1 & 0 & 0 & 0 \\ 0 & 0 & 0 & 0 & 0 & 0 & 1 & 0 & 0 \\ \frac{1}{\sqrt{3}} & 0 & 0 & \frac{1}{\sqrt{6}} & -\frac{1}{\sqrt{2}} & 0 & 0 & 0 & 0 \\ \frac{1}{\sqrt{3}} & 0 & 0 & \frac{1}{\sqrt{6}} & \frac{1}{\sqrt{2}} & 0 & 0 & 0 & 0 \\ \frac{1}{\sqrt{3}} & 0 & 0 & -\frac{2}{\sqrt{6}} & 0 & 0 & 0 & 0 & 0 \\ 0 & 0 & \frac{1}{\sqrt{3}} & 0 & 0 & 0 & 0 & -\frac{1}{\sqrt{6}} & \frac{1}{\sqrt{2}} \\ 0 & 0 & \frac{1}{\sqrt{3}} & 0 & 0 & 0 & 0 & -\frac{1}{\sqrt{6}} & -\frac{1}{\sqrt{2}} \\ 0 & 0 & \frac{1}{\sqrt{3}} & 0 & 0 & 0 & 0 & \frac{2}{\sqrt{6}} & 0 \end{pmatrix}. \quad (\text{A6})$$

Using Eqs. (A1), (A3), and (A6) the T_d normal mode Hamiltonian can be formulated in the C_{3v} point group and further converted into the ITO formalism through a six-mode tensor coupling scheme. Note that the passage in C_s is straightforward accounting for the group-subgroup *irrep* reduction $(A_1, E_a) \rightarrow (A', A')$ and $(A_2, E_b) \rightarrow (A'', A'')$.

As previously mentioned most of the currently published variational computer codes do not use the full T_d symmetry point group for dealing with methane-type molecules. Strictly speaking only one of its subgroup is employed and thus calculations could be more demanding. For example, our Contact Transformation procedure⁸⁸ which was recently applied for $^{12}\text{CH}_4$ was not originally implemented in the tetrahedral ITO formalism. Consequently the resulting *ab initio* effective Hamiltonian was not directly compatible with available computational programmes⁹⁰ of the spectra analyses and experimental fitting written in the ITO formalism. Using the transformations described in this paper, we are now able converting any rotation-vibration operator of methane isotopologues into a symmetry-adapted form. As a simple illustration we give the correspondence between the C_{3v} components and the T_d ITOs of Ref. 25 for two operators,

$$\left\{ [a_1^{(E)}]^2 \right\}_{C_{3v}} \rightarrow \sqrt{\frac{2}{3}} V^{(A_1)} + \frac{1}{\sqrt{3}} V^{(E)} + \frac{2}{3} \left(V_x^{(F_2)} + V_y^{(F_2)} - \frac{1}{2} V_z^{(F_2)} \right), \quad (\text{A7})$$

where using the nomenclature of Ref. 25:

$$\begin{aligned} V^{(A_1)} &= V_{\{0\}\{(2)_3\}}^{(A_1 A_1)_3 A_1 A_1 A_1 (A_1)} \\ V^{(E)} &= V_{\{0\}\{(2)_3\}}^{(A_1 E)_3 A_1 E A_1 E (E)} \\ V_{\sigma}^{(F_2)} &= V_{\{0\}\{(11)_3\}}^{(A_1 F_2)_3 A_1 F_2 A_1 F_2 (F_2)} \end{aligned} \quad (\text{A8})$$

and

$$\begin{aligned} & \left\{ -i [a^{(A_1)}]^2 J_x \right\}_{C_{3v}} \\ & \rightarrow -\frac{1}{3} T_{12}^{(E)} - \frac{5}{3\sqrt{3}} \left(T_{1x}^{(F_1)} + T_{1y}^{(F_1)} - \frac{1}{5} T_{1z}^{(F_1)} \right) \\ & \quad - \frac{1}{2\sqrt{3}} \left(T_{1x}^{(F_2)} - T_{1y}^{(F_2)} \right) + \frac{1}{6} \left(T_{2x}^{(F_1)} + T_{2y}^{(F_1)} - 2T_{2z}^{(F_1)} \right) \end{aligned} \quad (\text{A9})$$

with

$$\begin{aligned} T_{1\sigma}^{(C)} &= \left(V_{\{0\}\{(11)_4\}}^{(A_1 F_2)_4 A_1 A_1 F_2 (F_2)} \otimes R^{1(1, F_1)} \right)_{\sigma}^{(C)} \\ T_{2\sigma}^{(F_1)} &= \left(V_{\{0\}\{(2)_4\}}^{(A_1 A_1)_4 A_1 A_1 A_1 (A_1)} \otimes R^{1(1, F_1)} \right)_{\sigma}^{(F_1)}. \end{aligned} \quad (\text{A10})$$

Such relations are useful in the derivation of Hamiltonian or dipole moment operators.

- ¹M. Khalil, *Annu. Rev. Energy Environ.* **24**, 645 (1999).
- ²C. A. Nixon, B. Temelso, S. Vinatier, N. A. Teanby, B. Bézard, R. K. Achterberg, K. E. Mandt, C. D. Sherrill, P. G. J. Irwin, D. E. Jennings, P. N. Romani, A. Coustenis, and F. M. Flasar, *Astrophys. J.* **749**, 159 (2012).
- ³G. Tinetti, A. Vidal Madjar, D. Liang, J. P. Beaulieu *et al.*, *Nature* **448**, 169 (2007).
- ⁴M. R. Swain, P. Deroo, C. A. Griffith, G. Tinetti *et al.*, *Nature* **463**, 637 (2010).
- ⁵R. J. Hargreaves, C. A. Beale, L. Michaux, M. Irfan, and P. F. Bernath, *Astrophys. J.* **757**, 46 (2012).
- ⁶P. G. J. Irwin, C. de Bergh, R. Courtin, B. Bézard, N. A. Teanby, G. R. Davis, L. N. Fletcher, G. S. Orton, S. B. Calcutt, D. Tice, and J. Hurley, *Icarus* **220**, 369 (2012).
- ⁷C. D. Bergh, R. Courtin, B. Bézard, A. Coustenis, E. Lellouch, M. Hirtzig, P. Rannou, P. Drossart, A. Campargue, S. Kass, L. Wang, V. Boudon, A. Nikitin, and V. Tyuterev, *Planet Space Sci.* **61**, 85 (2012).
- ⁸L. A. Sromovsky, P. M. Fry, V. Boudon, A. Campargue, and A. Nikitin, *Icarus* **218**, 1 (2012).
- ⁹G. Tinetti, T. Encrenaz, and A. Coustenis, *Astron. Astrophys. Rev.* **21**, 63 (2013).
- ¹⁰M. Rey, A. V. Nikitin, and V. G. Tyuterev, *ApJ* **789**, 1 (2014).
- ¹¹Y. Lu, D. Mondelain, S. Kass, and A. Campargue, *J. Quant. Spectrosc. Radiat. Transfer* **112**, 2683 (2011).
- ¹²R. Beer and F. W. Taylor, *Astrophys. J.* **219**, 763 (1978).
- ¹³C. D. Parkinson, L. Ben-Jaffel, and J. C. McConnell, *Bull. Am. Astron. Soc.* **33**, 1042 (2001).
- ¹⁴R. Marquardt and M. Quack, *J. Chem. Phys.* **109**, 10628 (1998).
- ¹⁵R. Marquardt and M. Quack, *J. Phys. Chem. A* **108**, 3166 (2004).
- ¹⁶D. W. Schwenke and H. Partridge, *Spectrochim. Acta A* **57**, 887 (2001).
- ¹⁷D. W. Schwenke, *Spectrochim. Acta A* **58**, 849 (2002).
- ¹⁸T. Carrington, Jr., *Can. J. Chem.* **82**, 900 (2003).
- ¹⁹X. G. Wang and T. Carrington, Jr., *J. Chem. Phys.* **121**, 2937 (2004).
- ²⁰X. G. Wang and T. Carrington, Jr., *J. Chem. Phys.* **119**, 101 (2003).
- ²¹X. G. Wang and E. L. Sibert III, *J. Chem. Phys.* **111**, 4510 (1999).
- ²²X. G. Wang and E. L. Sibert III, *Spectrochim. Acta, Part A* **58**, 863 (2002).
- ²³P. Cassam-Chenaï, Y. Bouret, M. Rey, S. A. Tashkun, A. V. Nikitin, and V. G. Tyuterev, *Int. J. Quantum Chem.* **112**, 2201 (2012).
- ²⁴D. A. Sadovskii, D. N. Kozlov, and P. P. Radi, *Phys. Rev. A* **82**, 012503 (2010).
- ²⁵M. Rey, A. V. Nikitin, and V. G. Tyuterev, *J. Chem. Phys.* **136**, 224106 (2012).
- ²⁶A. V. Nikitin, M. Rey, and V. G. Tyuterev, *Chem. Phys. Lett.* **501**, 179 (2011).
- ²⁷P. Cassam-Chenaï and J. Liévin, *J. Chem. Phys.* **136**, 174309 (2012).
- ²⁸R. Warmbier, R. Schneider, A. R. Sharma, B. J. Braams, J. M. Bowman, and P. H. Hauschildt, *Astron. Astrophys.* **495**, 655 (2009).
- ²⁹M. Rey, A. V. Nikitin, and V. G. Tyuterev, *J. Mol. Spectrosc.* **291**, 85 (2013).
- ³⁰M. Rey, A. V. Nikitin, and V. G. Tyuterev, *Phys. Chem. Chem. Phys.* **15**, 10049 (2013).

- ³¹H. Hollenstein, R. R. Marquardt, M. Quack, and M. Suhm, *J. Chem. Phys.* **101**, 3588 (1994).
- ³²X. G. Wang and T. Carrington, Jr., *J. Chem. Phys.* **123**, 154303 (2005).
- ³³J. W. Perry, D. J. Moll, A. Kuppermann, and A. H. Zewail, *J. Chem. Phys.* **82**, 1195 (1985).
- ³⁴K. E. Deng, X. G. Wang, H. Lin, D. Wang, and Q. Zhu, *Mol. Phys.* **97**, 787 (1999).
- ³⁵L. Halonen and M. S. Child, *Mol. Phys.* **46**, 239 (1982).
- ³⁶L. Halonen and M. S. Child, *Comput. Phys. Commun.* **51**, 173 (1988).
- ³⁷G. A. Voth, R. A. Marcus, and A. H. Zewail, *J. Chem. Phys.* **81**, 5494 (1984).
- ³⁸P. Jensen, *Mol. Phys.* **98**, 1253 (2000).
- ³⁹G. Tarrago, M. Delaveau, L. Fusina, and G. Guelachvili, *J. Mol. Spectrosc.* **126**, 149 (1987).
- ⁴⁰C. B. Suárez, *Spectrosc. Lett.* **28**, 429 (1995).
- ⁴¹A. Nikitin, J. P. Champion, V. G. Tyuterev, L. R. Brown, G. Mellau, and M. Lock, *J. Mol. Struct.* **517–518**, 1 (2000).
- ⁴²A. Nikitin, L. R. Brown, L. Féjard, J. P. Champion, and V. G. Tyuterev, *J. Mol. Spectrosc.* **216**, 225 (2002).
- ⁴³L. R. Brown, A. Nikitin, D. Chris Banner, V. Malathy Devi *et al.*, *J. Mol. Struct.* **695–696**, 181 (2004).
- ⁴⁴A. Nikitin, J. P. Champion, and L. R. Brown, *J. Mol. Spectrosc.* **240**, 14 (2006).
- ⁴⁵A. V. Nikitin, L. R. Brown, K. Sung, M. Rey, V. G. Tyuterev, M. A. H. Smith, and A. W. Mantz, *J. Quant. Spectrosc. Radiat. Transfer* **114**, 1 (2013).
- ⁴⁶L. S. Rothman, I. E. Gordon, Y. Babikov, A. Barbe *et al.*, *J. Quant. Spectrosc. Radiat. Transfer* **130**, 4 (2013).
- ⁴⁷L. R. Brown, K. Sung, D. C. Benner, V. M. Devi *et al.*, *J. Quant. Spectrosc. Radiat. Transfer* **130**, 201 (2013).
- ⁴⁸A. V. Nikitin, O. M. Lyulin, S. N. Mikhailenko, V. I. Perevalov *et al.*, *J. Quant. Spectrosc. Radiat. Transfer* **111**, 2211 (2010).
- ⁴⁹A. Campargue, O. Leshchishina, L. Wang, D. Mondelain, and S. Kassi, *J. Mol. Spectrosc.* **291**, 16 (2013).
- ⁵⁰O. N. Ulenikov, E. S. Bekhtereva, S. Albert, S. Bauerecker, H. Hollenstein, and M. Quack, *Mol. Phys.* **108**, 1209 (2010).
- ⁵¹Y. Perez Delgado, E. L. Lewis, C. J. Moehnke, M. C. Salazar, A. J. Hernandez, and C. E. Manzanarez, *Mol. Phys.* **107**, 1367 (2009).
- ⁵²H. Partridge and D. W. Schwenke, *J. Chem. Phys.* **106**, 4618 (1997).
- ⁵³T. Cours, P. Rosmus, and V. G. Tyuterev, *J. Chem. Phys.* **117**, 5192 (2002).
- ⁵⁴O. Polyansky, A. Császár, S. Shirin, N. Zobov, P. Barletta, J. Tennyson, D. Schwenke, and P. Knowles, *Science* **299**, 539 (2003).
- ⁵⁵V. G. Tyuterev, L. Régalia-Jarlot, D. W. Schwenke, S. A. Tashkun, and Y. G. Borkov, *C. R. Phys.* **5**, 189 (2004).
- ⁵⁶A. Nikitin, F. Holka, V. G. Tyuterev, and J. Fremont, *J. Chem. Phys.* **130**, 244312 (2009).
- ⁵⁷S. Yurchenko, J. Zheng, H. Lin, P. Jensen, and W. Thiel, *J. Chem. Phys.* **123**, 134308 (2005).
- ⁵⁸X. Huang, D. W. Schwenke, and T. J. Lee, *J. Phys. Chem. A* **113**, 11954 (2009).
- ⁵⁹S. Carter, A. R. Sharma, J. Bowman, P. Rosmus, and R. Tarroni, *J. Chem. Phys.* **131**, 224106 (2009).
- ⁶⁰P. Barletta, S. V. Shirin, N. F. Zobov, O. L. Polyansky, J. Tennyson, E. F. Valeev, and A. G. Császár, *J. Chem. Phys.* **125**, 204307 (2006).
- ⁶¹P. G. Szalay, F. Holka, J. Fremont, M. Rey, K. A. Peterson, and V. G. Tyuterev, *Phys. Chem. Chem. Phys.* **13**, 3654 (2011).
- ⁶²F. Holka, P. G. Szalay, J. Fremont, M. Rey, K. A. Peterson, and V. G. Tyuterev, *J. Chem. Phys.* **134**, 094306 (2011).
- ⁶³M. Pavanello, L. Adamowicz, A. Alijah, N. F. Zobov, I. I. Mizus, O. L. Polyansky, J. Tennyson, T. Szidarovszky, and A. G. Császár, *J. Chem. Phys.* **136**, 184303 (2012).
- ⁶⁴V. G. Tyuterev, R. Kochanov, S. Tashkun, F. Holka, and P. G. Szalay, *J. Chem. Phys.* **139**, 134307 (2013).
- ⁶⁵A. V. Nikitin, X. Thomas, L. Régalia, L. Daumont, P. Von der Heyden, V. G. Tyuterev, L. Wang, S. Kassi, and A. Campargue, *J. Quant. Spectrosc. Radiat. Transfer* **112**, 28 (2011).
- ⁶⁶A. V. Nikitin, M. Rey, and V. G. Tyuterev, *Chem. Phys. Lett.* **565**, 5 (2013).
- ⁶⁷M. Rey, A. V. Nikitin, and V. G. Tyuterev, *Mol. Phys.* **108**, 2121 (2010).
- ⁶⁸C. Eckart, *Phys. Rev.* **47**, 552 (1935).
- ⁶⁹J. D. Louck and H. W. Galbraith, *Rev. Mod. Phys.* **48**, 69 (1976).
- ⁷⁰L. C. Biedernharn and J. D. Louck, *Angular Momentum in Quantum Physics* (Cambridge University Press, New York, 1985).
- ⁷¹F. O. Meyer III and R. W. Redding, *J. Mol. Spectrosc.* **70**, 410 (1978).
- ⁷²R. W. Redding and F. O. Meyer III, *J. Mol. Spectrosc.* **74**, 486 (1979).
- ⁷³E. B. Wilson, J. C. Decius, and P. C. Cross, *Molecular Vibrations* (McGraw-Hill, New York, 1955).
- ⁷⁴P. R. Bunker and P. Jensen, *Molecular Symmetry and Spectroscopy* (NRC-CNRC, Ottawa, 1998).
- ⁷⁵A. R. Hoy, I. M. Mills, and G. Strey, *Mol. Phys.* **24**, 1265 (1972).
- ⁷⁶M. R. Aliev, and J. K. G. Watson, in *Higher-Order Effects in the Vibration-Rotation Spectra of Semirigid Molecules*, edited by K. N. Rao (Academic Press, London, 1985).
- ⁷⁷J. G. Watson, *Mol. Phys.* **15**, 479 (1968).
- ⁷⁸T. J. Lee, J. M. L. Martin, and P. R. Taylor, *J. Chem. Phys.* **102**, 254 (1995).
- ⁷⁹J. K. G. Watson, *J. Mol. Spectrosc.* **228**, 645 (2004).
- ⁸⁰B. T. Sutcliffe in *Coordinate Systems and Transformations*, edited by S. Wilson (John Wiley & Sons, 2003).
- ⁸¹J. D. Louck, *J. Mol. Spectrosc.* **61**, 107 (1976).
- ⁸²W. Thiel, *Mol. Phys.* **68**, 427 (1989).
- ⁸³Y. Makushkin and O. Ulenikov, *J. Mol. Spectrosc.* **68**, 1 (1977).
- ⁸⁴B. Crawford, Jr., *J. Chem. Phys.* **20**, 977 (1952).
- ⁸⁵B. P. Winnewisser and J. K. G. Watson, *J. Mol. Spectrosc.* **205**, 227 (2001).
- ⁸⁶A. D. Bykov, Y. S. Makushkin, and O. N. Ulenikov, *J. Mol. Spectrosc.* **93**, 46 (1982).
- ⁸⁷See supplementary material at <http://dx.doi.org/10.1063/1.4890956> for the complete line list of $^{12}\text{CH}_3\text{D}$ up to 5000 cm^{-1} and for the potential force constants in C_{3v} symmetry coordinates.
- ⁸⁸V. G. Tyuterev, S. Tashkun, M. Rey, R. Kochanov, A. V. Nikitin, and T. Delahaye, *J. Phys. Chem. A* **117**, 13779 (2013).
- ⁸⁹A. V. Nikitin, J. P. Champion, and V. G. Tyuterev, *J. Mol. Spectrosc.* **182**, 72 (1997).
- ⁹⁰A. V. Nikitin, M. Rey, J. P. Champion, and V. G. Tyuterev, *J. Quant. Spectrosc. Radiat. Transfer* **113**, 1034 (2012).
- ⁹¹J. Moret-Bailly, *Cah. Phys.* **15**, 237 (1961).
- ⁹²B. Zhilinskii, *Opt. Spectrosc.* **51**, 262 (1981).
- ⁹³S. N. Yurchenko, W. Thiel, and P. Jensen, *J. Mol. Spectrosc.* **245**, 126 (2007).
- ⁹⁴G. Avila and T. Carrington, Jr., *J. Chem. Phys.* **135**, 064101 (2011).
- ⁹⁵S. Carter, A. R. Sharma, and J. M. Bowman, *J. Chem. Phys.* **137**, 154301 (2012).
- ⁹⁶C. Fábri, E. Mátyus, T. Furtenbacher, L. Nemes, B. Mihály, T. Zoltáni, and A. Császár, *J. Chem. Phys.* **135**, 094307 (2011).
- ⁹⁷A. Császár, C. Fábri, T. Szidarovszky, E. Mátyus, T. Furtenbacher, and G. Czako, *Phys. Chem. Chem. Phys.* **14**, 1085 (2012).
- ⁹⁸J.-Q. Chen, J. Ping, and F. Wang, *Group Representation Theory for Physicists*, 2nd ed. (World Scientific, Singapore, 2002).